Title: Exploring novel active metabolite and repurposing old drug to combat cardiometabolic diseases

Authors: Malladi Navya, Sanjay K Banerjee

1. Introduction:

Cardiometabolic disease (CMD) is a spectrum of diseases that include insulin resistance, metabolic syndrome, pre-diabetes, and more severe illnesses like cardiovascular disease (CVD) and type 2 diabetes (T2DM)(1). Globally, CMDs constitute the leading cause of death. Poor lifestyle habits such as physical inactivity, smoking, and a poor diet, are the primary risk factors for CMD (2). Numerous cardiometabolic problems, such as dyslipidemia, obesity, type 2 diabetes, hypertension, nephropathy, and nonalcoholic fatty liver disease, are intricately linked to one another (3). CMD has a complex phenotype that results from the interactions of genetic, environmental, and dietary variables (4). T2DM is one of the most prevalent among CMDs which puts people at higher risk for developing diabetic cardiomyopathy and atherosclerotic cardiovascular disease (CVD), both of which can cause heart failure through several different mechanisms, such as myocardial infarction and chronic pressure overload. (5).

The central mechanism for these cardiovascular complications in diabetes includes an imbalance in the systems that maintain the homeostasis of blood coagulation and fibrinolysis [7]. This imbalance results in diabetic thrombocytopathy (6), a condition majorly affects platelet function and ultimately results in heart attacks or stroke in diabetes (7–9). Scientific research has shown that antiplatelet therapy can reduce cardiovascular complications in diabetes and premature death (10,11). Despite having many drugs and therapies for the management of diabetes, it is still under the category of a life-threatening disease because of its complications. Further various research has reported an increasing adverse reaction in patients using anti-diabetes drugs for the long term (12). This has made an immense impact on scientific researchers for exploring new strategies for diabetic treatment having the least adverse reactions. Dietary therapy in diabetes is one of them showing a tremendous effect on preventing and controlling diabetes(13). Among large numbers of nutritional diets, garlic has been showing a very promising effect on diabetes as well as diabetic complications (14–16). An antiplatelet property has been observed in raw garlic, preventing cardiovascular complications in diabetes (17,18). Scientific literature strongly supports that garlic is showing these beneficial effects mainly due to its sulfur-containing compounds (19,20). Allyl methyl sulfide (AMS), an active metabolite observed inside the body after oral administration of raw garlic shown effects on diabetes by reducing glucose levels, increasing insulin levels, and reducing hepatic oxidative stress caused by glucotoxicity in diabetes (21,22). Moreover, we have previously shown the beneficial effect

of AMS on attenuating hypertrophy in rats (23,24). However, the effect of AMS on diabetic complications in thrombosis especially on platelet activation and aggregation yet to be reported.

Similarly, NAFLD is a phenotype of the cardiometabolic syndrome (25). NAFLD is a condition of the liver with excessive accumulation of fats in the hepatocytes (26). The pathophysiology of NAFLD involves several pathways which interlinked in a complex way and therefore, make the disease difficult to understand (27). There is abundant evidence of a direct link between NAFLD and multiple cardio-metabolic disorders including ischemic stroke, insulin resistance, hypertension, chronic kidney disease (CKD), and cardiac arrhythmias (28,29). Along with the increasing heterogenicity of NAFLD pathophysiology, the lack of effective treatment in NAFLD highlights the need for exploring more therapeutic strategies in NAFLD (30).

Cardiometabolic disorders such as NAFLD and vitamin D deficiency are becoming increasingly more prevalent across multiple populations (31,32). Previous studies showed that vitamin D (fat-soluble vitamin) can affect the liver through the Vitamin D receptor (VDR) (33,34). VDR is present in hepatic cells, and its expression can reduce inflammation in chronic hepatic diseases (35). Vitamin D analog, paricalcitol has shown a beneficial role in diseases like chronic kidney injury, cholestatic liver injury, and hepatitis B (36–38). However, the role of paricalcitol in chronic liver diseases such as NAFLD is still not explored yet.

Therefore, in this present study, we aim to explore the therapeutic strategies which either derived from a natural source or an FDA-approved drug for cardiometabolic diseases such as diabetes as well as NAFLD. We tried to understand the therapeutic benefits of garlic metabolite, Allyl Methyl Sulfide on altered parameters of diabetic platelets. Similarly, we have evaluated the effect of paricalcitol, an FDA-approved drug for chronic kidney disease, in modulating inflammation and oxidative stress by decreasing the acetylation of hepatic proteins in NAFLD as well as in improving cardiac function.

2. Objective:

2.1. Finding the role of allyl methyl sulfide, an active metabolite of garlic, in the activation of platelets of diabetes mellitus

METHOD: Animals study, Cell culture, Blood collection and isolation of platelets, Measuring the number of activated platelets by flow cytometer, Measuring platelet aggregation in the presence of ADP, a platelet agonist, by flow Cytometry, Platelet and macrophage interaction, Measurement of endogenous ROS in platelets

2.2. Finding the therapeutic efficacy of paricalcitol, a vitamin D analog in a rat model of NAFLD.

METHOD: NAFLD rat model development, biochemical analysis of serum, histopathology examination of liver, immunoprecipitation and western blotting of liver tissue protein, Gene expression profiling, lipid peroxidation assay, glutathione assay, catalase activity assay, DPPH (Total antioxidant) assay, DCFDA assay, echocardiography.

3. Material and Methods

OBJECTIVE 1- Finding the role of allyl methyl sulfide, an active metabolite of garlic, in the activation of platelets of diabetes mellitus.

3.1. Animals and Study Design

Wistar rats 200-250g were used to develop diabetes and evaluate the effect of AMS on platelet activation and aggregation. Animals were procured from Jeeva Life Sciences (Hyderabad, India). The study was approved by the Institutional Animal Ethics Committee (IAEC) of the National Institute of Pharmaceutical Education and Research (NIPER), Guwahati, India (NIPER/BT/2020/37). The animals were housed in individually ventilated cages (IVC) at an animal house facility of NIPER, Guwahati under standard conditions (temperature 23 ± 1°C, 50 ± 15 % relative humidity, and 12 h light/dark cycle). Wistar rats were allowed free access to food and water ad libitum during the study. Post seven days of acclimatization, animals were randomly allocated into four groups (n = 6): Group 1: control, Group 2: Diabetes (STZ 35mg/kg), Group 3: Diabetes + AMS (50 mg/kg), and Group 4: Diabetes + Aspirin (30 mg/kg). All these rats were maintained for 10 weeks. Every week the body weight of all animals was recorded to understand the body weight gain or loss during the experimental period as well as and glucose levels were monitored by using a glucometer (Accu Chek Active, Roche). The doses of AMS and Aspirin were chosen from our previous work and scientific literature (23,39).

3.2. Cell culture

Human macrophages (THP-1 cells; an acute monocytic leukemia cell line) were a kind gift from Translational Health Science and Technology (THSTI, Faridabad, India). The cells were cultured in RPMI 1640 medium enriched with fetal bovine serum (10% v/v), and anti-microbial agents (antibiotic and antimycotic) (100U/ml) and cultured under standard conditions that are 37°C and 5% CO_2 incubator (Eppendorf CellXpert C170)

3.3. Blood collection and isolation of platelets

The platelets were isolated from blood by dual centrifugation. It has been carried out at room temperature. Preventive measures have been taken to avoid platelet activation during the process. Initially, the animals were anesthetized with the help of isoflurane. Through retroorbital plexus using a capillary tube, blood was collected into a tube containing 3.8% sodium citrate (9:1 ratio) and centrifuged at 500 rpm for 15 minutes at 20°C temperature. The centrifugation results in the isolation of platelet-rich plasma (PRP) as the upper layer in a tube. Almost $3/4^{th}$ of this layer was taken into a fresh tube using a wide-bore pipette tip. Further platelets were pelleted by centrifuging the PRP at 400g for 10

minutes at 20°C. The platelets pellet was washed, resuspended in HEPES-Tyrode buffer, and stored at -80°C.

3.4. Measuring the number of activated platelets by flow cytometer

The *in vivo* activated status of isolated platelets was measured by flow cytometry using fluorochrome-tagged antibodies. All these works were carried out within 2 hours of blood collection and all measures to avoid platelet activation during the handling of the sample. Seven µl of PRP was taken in a tube and diluted by adding 50 µl of HEPES-Tyrode's buffer having 1% BSA. Samples were added with antibody mix having FITC anti-mouse/rat CD61 antibody (platelet surface marker) and APC anti-mouse/rat CD62P antibody (platelet activation marker) diluted with HEPES-Tyrode's buffer (with 1% BSA). Stained platelets were incubated in the dark for 30 minutes at room temperature. Immediately analyzed the samples by using Attune™ NxT Flow Cytometer, where analysis was done by taking 50,000 events for each sample. The compensation was done using individual antibody-stained cells and unstained cells to avoid spillover from one channel to another. Platelets were gated on forward light scatter (FSC) vs. side light scatter (SSC) plot and the percentage of CD62P positive cells are enumerated among platelets positive CD61 cells which gives % activated platelets.

3.5. Measuring platelet aggregation in the presence of ADP, a platelet agonist, by flow cytometry

With a few modifications to the previously mentioned procedure, the hypersensitivity of platelets in the presence of platelet-aggregating agents (ADP) has been observed by measuring the percentage aggregation of platelets by flow cytometry (40). Fifty µl of freshly isolated platelet-rich plasma (PRP) was resuspended in 450 µl of HEPES-Tyrode buffer. Platelets were activated by adding 20 µM ADP as a final concentration and incubated for 10 minutes at 37 °C under shaking conditions at 1000rpm using a thermo shaker. Diluted PRP without agonist was used as a negative control. Cells were analyzed by flow cytometry for the presence of platelet aggregation. Platelets were differentiated from platelet aggregated by gating cells on forward light scatter (FSC) versus side light scatter (SSC) plots where the platelet aggregates have increased size and density.

3.6. Platelet and macrophage interaction

The heterogeneous interactions of platelets with macrophages were analyzed by flow cytometry method using phorbol 12-myristate 13-acetate (PMA) differentiated THP-1 macrophages (41,42).

Monocyte differentiation to macrophage: THP-1 is a human monocytic cell line. THP-1 monocytes (1.5×10^6 cells) were seeded in 6 well plates having 1ml of Roswell Park Memorial Institute medium (RPMI-1640) which was supplemented with 100 µg/ml streptomycin, 100 U/ml penicillin, and 10% fetal calf

serum. The monocytes were differentiated to macrophages by adding 50 ng phorbol 12-myristate 13-acetate (PMA) and incubated for 48 hours in an incubator maintaining 5% CO_2 at 37 °C under humidified conditions. After 48 hours of incubation, the media is changed to fresh RPMI-1640 complete media without the addition of PMA and incubated for 48 hours in an incubator.

Macrophage and platelet co-culture study: Isolated PRP of 7 µl was added to a culture plate having macrophages derived from THP1 and incubated for 30 minutes in a CO_2 incubator. After successive co-culturing of platelets, each well was washed with PBS to remove floating platelets. Cells were trypsinized by adding 0.25% trypsin EDTA and incubated in a CO_2 incubator for 2 minutes. The detached cells were collected in an individual tube and centrifuged at 400g for 10 minutes at 20°C. The supernatant was discarded; the pellet was washed with PBS and fixed by incubating with 4% paraformaldehyde for 10 minutes. The cells further were washed and resuspended in PBS for labeling with fluorescently conjugated antibodies of macrophage surface marker (CD14 PE) and platelet-specific marker (CD61 FITC). The cells were incubated in the dark for 30 minutes at room temperature and analyzed by Attune™ NxT Flow Cytometer. Analysis was done by gating the macrophage population under the FSC vs. SSC plot. To compensate for the overlapping spectra single stained cells were used. Finally, we generated a mean fluorescence intensity (FITC)/cell count plot for macrophage positive for CD14 marker.

3.7. Measurement of endogenous ROS in platelets

Intracellular ROS was measured by using 2',7'-dihydro dichlorofluorescein diacetate, and H_2DCFDA dye as per the procedures mentioned in articles (43,44). The freshly isolated PRP (7.0 µl) was diluted in 100 µl of HEPES- Tyrode's buffer and incubated with 10 µM of H_2DCFDA dye under dark conditions for 30 min at 37 °C. Later samples were further diluted with 200 µl HEPES-Tyrode's buffer and mixed gently with a pipette. The tubes were centrifuged at 400g for 10 minutes at 20°C for pelleting the cells and discarding the supernatant. Further resuspended the pellet by adding 100 µl of HEPES-Tyrode's buffer. The unstained samples were used as a negative control. All of these samples were analyzed using Attune™ NxT Flow Cytometer by taking 10,000 events where the mean fluorescent intensity of DCFDA in platelets population was determined for each sample.

3.8. Metabolomics sample preparation and data acquisition

To the cell pellet, 10µl of isotope-labeled internal standards cocktail/mixture was added. The macromolecules were precipitated by performing the extraction with 750µl cold mixture of methanol: water (4:1). Then the extracted samples were vortexed vigorously followed by the addition of 450µl of chilled chloroform with vortexing for 5min and further addition of 150µl of milli-Q water with vortexing

for 3mins. The whole mixture was kept in a freezer (-20°C, ~30min) followed by centrifugation at 5000 rpm (2491 × g) for 10min at 4°C. Both layers containing the extracted metabolites and internal standards were evaporated to dryness, reconstituted in acetonitrile: water (1:1) mixture, and subjected to LC-MS/MS analysis. A Jet Stream electrospray ionization mode (Agilent AJS ESI) was employed for the ionization of the analytes in both positive and negative modes. The source gas temperature was set to 290°C, gas flow 13l/min, nebulizer 50 psi, sheath gas temperature 50°C, sheath gas flow 250°C, capillary voltage +4500 for positive and - 4500 for negative. The separation of the metabolites was achieved on ShodexAsahipak NH2P-40 2D (150mm x 2mm, 4µm) held at 35°C for chromatographic separation. The mobile phase was solvent solvent A: 95% water with 20mM (NH4)2CO3, 5% acetonitrile, and 38mM NH4OH, final pH 9.75, and solvent B: 100% acetonitrile. Separation was achieved using the following gradient: 0-3.5min: 95% B, 3.6-8min: 85% B, 8.1-13min: 75% B, 13.5–35min: 0% B, 36–46min: 95% B, 46.1min: end. The flow rate was 0.2ml/min. The injection volume was 10µl. All the samples were kept at 4°C during analysis.

OBJECTIVE 2- Finding the therapeutic efficacy of paricalcitol, a vitamin D analog in a rat model of NAFLD.

3.9. Animal experiment design

We have received approval from the Institutional Animal Ethical Committee Approval (IAEC), NIPER-Guwahati to conduct the animal experiment (NIPER/BT/2020/01). NAFLD was induced by feeding a choline-deficient high-fat (CDHF) diet in male Sprague-Dawley rats (weight: 200-250g) (NAFLD group) for 20 weeks. Animals were monitored every week till 20 weeks for their body weight change and food intake. A corresponding number of weight-matched rats (Control group) were maintained as controls and fed with the chow diet. After 12 weeks of CDHF diet feeding, Paricalcitol 0.08ug /kg/day according to their body weight was administered to the NAFLD rats (NAFLD + PCAL group) for up to 8 weeks (from 12 to 20 weeks). Paricalcitol solution was prepared by dissolved in propylene glycol: ethanol and diluted further with PBS to administer in rats via the intraperitoneal (IP) route at a dose of 0.08ug/kg/day.

3.10. Histopathology examination

After 20 weeks of the study, the liver tissue was subjected to histopathology to observe the morphological changes. Briefly, whole liver tissue was excised and cleaned with ice-cold then fixed in the 4 % formalin, routinely processed, and embedded into paraffin. Paraffin sections were cut into 5 µm thick sections and mounted in a glass slide then stained with hematoxylin and eosin (H& E) stain and examined under a light microscope (EVOS, ThermoFisher Scientific, USA).

3.11. Biochemical analysis

Animals were numbed using isoflurane, and blood samples were drawn through the retro-orbital puncture. Serum was isolated and used to analyze various serum parameters such as total cholesterol, triglycerides (TG), low-density lipoprotein (LDL), high-density lipoprotein (HDL), and uric acid using Randox biochemical analyzer. Serum alanine transaminase (ALT) and aspartate transaminase (AST) were measured using biochemical assay kits. While insulin level in serum was measured using an ELISA kit.

3.12. Immunoprecipitation and western blotting

Immunoprecipitation was performed by using an immunoprecipitation kit. Five mg of liver tissue incubated with 2.0 µl of anti-acetylated lysin antibody. Following antibody (anti-acetylated lysine antibody) binding, the acetylated protein precipitated by adding 25 µl of Protein A/G Sepharose beads slurry. Further immunoblotting was performed with precipitated proteins against FOXO3A, and NFκB to see individual protein acetylation. Similarly, whole protein lysates were used to perform immunoblotting against acetylated lysin, SIRT1, SIRT3, FOXO3A, and NFκB (45,46). Stain-free gel or GAPDH was used as a loading control for all the immunoblotting studies.

3.13. Gene expression profiling

RNA was isolated from liver tissues of all groups using TRIzol reagent. Quantification and quality assessment of RNA was performed using a Spectrophotometer (Epoch Biotek microplate reader). cDNA was synthesized using 1mg of RNA and performed polymerase chain reaction (PCR) to know the expression of inflammatory genes i.e., TNF-α, IL1-β, and NFkB, and antioxidant genes i.e., catalase, MnSOD using Emerald GT PCR Master mix and respective primers (**Table 1**). The data were normalized to the expression of the housekeeping gene RPL32. The PCR image density was quantified using Image J software.

Table 1: List of primers

Primer name	Nucleotide sequence (5′-3′)	Product Length (bp)
RPL32	F: AGATTCAAGGGCCAGATCCT R: CGATGGCTTTTCGGTTCTTA	193 bp
IL-1β	F: CCAGGATGAGGACCCAAGCA R: TCCCGACCATTGCTGTTTCC	519 bp
TNF α	F: CGACTCTGACCCCCATTACT R: CGTCTCGTGTGTTTCTGAGC	153 bp
NFκB	F: GTGCAGAAAGAAGACATTGAGGTG R: AGGCTAGGGTCAGCGTATGG	131 bp
Catalase	F: GCGAATGGAGAGGCAGTGTAC R: GAGTGACGTTGTCTTCATTAGCACTG	652 bp
MnSOD	F: GAACCACAGGCCTTATTCCA R: GGGCTTCACTTCACTTCTTGCAAAC	161bp

3.14. Lipid peroxidation assay

As per the protocol mentioned by Ohkawa et.al (47), lipid peroxidation was performed by homogenizing liver tissue in 10% (w/v) of ice-cold 0.05 M potassium phosphate buffer (pH 7.4). Homogenate of 30 µl was combined with 0.8% thiobarbituric acid (TBA), 0.2 ml of 8.1% SDS, and 1.5 ml of 20% acetic acid. The volume was made with distilled water to 4.0 ml, and the solution was held in a water bath with a temperature of 95 °C for one hour. After centrifuging the supernatant was isolated and an equivalent volume of butanol: pyridine (15:1) was added to the supernatant. The optical density of the organic layer was assessed at 532 nm. Then the mM of MDA formed per mg of protein using a standard curve of 1,1,3,3-tetraethoxypropane at a different concentration.

3.15. Glutathione assay

The assay of glutathione was carried out using Ellman's technique (48). In short, 10% (w/v) of ice-cold 0.05 M potassium phosphate buffer (pH 7.4) was used to homogenize the liver tissues. The resulting homogenate was centrifuged at 14000 rpm for 20 minutes at 4°C and supernatant was collected. A hundred µl of supernatant was mixed with 500 µl of 5% trichloroacetic acid (TCA) and the mixture was centrifuged at 2,300 g for 10 min to deproteinize the sample. Further, 250 µl of dithiol-nitro-benzoic acid (DTNB) and 1.5 ml of 0.3 M disodium hydrogen phosphate were added to 100 µl of the deproteinized sample. At last,

the optical density of the prepared sample was measured at 412 nm and the results were calculated as a micromole of glutathione (GSH) present in mg of protein.

3.16. Catalase activity assay

Catalase assay was carried out using Aebi's method (49). In brief, 0.5 µl of the tissue supernatant prepared by homogenizing the liver tissue in 10% of 0.05M phosphate buffer was taken and added to 0.5 ml of 50 mM phosphate buffer (pH 7.0). Finally, the prepared sample mixture is added with 250 µl of 30 mM H_2O_2. The change in absorbance at 240 nm was monitored with a 15-second gap for 1.5 minutes. The catalase activity in the liver was measured as the rate of H_2O_2 oxidation per minute per milligram of protein.

3.17. DPPH (Total antioxidant) assay

Percentage antioxidant activity was measured using a 2,2-diphenylpicrylhydrazyl (DPPH) assay (50). Briefly, liver tissue was homogenized in 10% (w/v) of ice-cold 0.05 M potassium phosphate buffer (pH 7.4). DPPH solution was prepared at the concentration of 0.195 mg/ml in methanol. To 5 ul of tissue homogenate, 100 µl DPPH solution and 100 µl tris buffer were added. Further incubated for 30 minutes and absorbance was taken at 517nm by a microplate reader using methanol as blank. Free radical scavenging activity of the liver was measured through the obtained optical density readings. Lower optical density represents the higher antioxidant status in the liver.

3.18. DCFDA assay

Liver reactive oxygen species (ROS) was measured using 2, 7-dichlorofluorescein diacetate (DCF-DA) method (51), where 100 mM of DCF-DA was added to 5 µl of liver tissue homogenate and incubated for 30 min at room temperature in the dark. After incubation, phosphate buffer saline (PBS, 0.1 M, pH-7.4) was used to regulate the reaction's volume, and the fluorescence was measured at 488 nm excitation and 525 nm emission wavelengths using a multimode reader.

3.19. Myeloperoxidase assay

Myeloperoxidase (MPO) assay was performed using the Bradley protocol (52). In brief, the liver tissue homogenate was added to 5% hexadecyl trimethyl ammonium bromide (HTAB) and 10 mM EDTA. Then the homogenates were freeze-thawed followed by centrifuged at 13000 g for 20 min. The supernatant obtained was used for the estimation of MPO activity using 0.167 mg/ml of o-dianisidine hydrochloride and 0.005% hydrogen peroxide at 460 nm. The MPO activity was expressed as U/g of tissue.

3.20. Echocardiography of rats

Transthoracic echocardiography was performed with a 13MHz linear array transducer system (Vevo 3100). Rats were anesthetized with isoflurane(70mg/kg) and the chest hair was removed. The transducer was placed on the left hemothorax. Two dimensionally guided left ventricle (LV) M-mode images at the papillary muscle level were obtained from the parasternal short-axis view. Left ventricle posterior thickness, interventricular septal thickness, and LV internal dimensions at the end diastole and systole were measured from M-mode images. Fractional shortening (FS) of LV was calculated as follows: LV FS% = [(LVDd-LVSd)/LVDd]*100, where LVDd is LV dimension at end-diastole and LVSd is LV dimension at end-systole.

3.21. Statistical analysis

Statistical analysis was performed using Graph pad Prism (Graph Pad Software, San Diego, CA, USA). All statistical analyses were made by either means of unpaired student t-test (for comparison between two groups) or one-way ANOVA (for comparison among three or more groups). The data were represented as mean ± SEM. $P < 0.05$ is considered significant. Metaboanlyst 5.0 was used to analysis the metabolomics data as well as for pathway analysis,

4. Results

OBJECTIVE 1- Finding the role of allyl methyl sulfide, an active metabolite of garlic, in the activation of platelets of diabetes mellitus.

4.1. Body weight and blood glucose level changes in rats

We monitored the body weights and blood glucose levels of experimental rats until 10 weeks. The mean values of body weight in grams of all study groups were compared in the 0^{th}, 3^{rd}, $7^{th,}$ and 10^{th} week and plotted as bar graphs. As shown in Figure 1A, we did not observe any significant changes among all four groups. The blood glucose levels of the diabetes group significantly increased at all the time points when compared to the control. However, AMS treatment decreased the glucose levels at 7 and 10 weeks when compared to the 0^{th} and 3^{rd} week of treatment (Figure 1B).

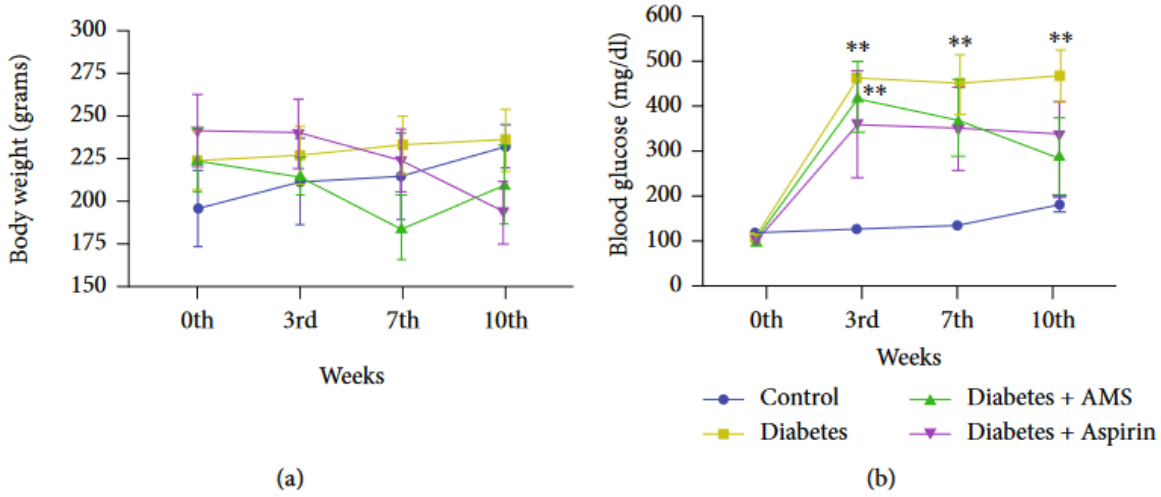

Figure 1: (A) Body weights and (B) Blood glucose levels of control, diabetes, AMS-treated, and aspirin-treated rats at the end of 0^{th}, 3^{rd}, $7^{th,}$ and 10^{th} weeks. All values are represented as mean ± SEM (N= 4-6). *$p < 0.05$, ** $p < 0.01$ vs control.

4.2. Effect of AMS on platelet activation in diabetes

The *in vivo* activated status of platelets in control, diabetes, and treatment groups after the 3^{rd} and 10^{th} weeks of study duration has been analyzed by flow cytometry. The graph represents the percent CD61 positive (CD61+) on the X-axis and CD62P positive platelets on the Y-axis (Figure 2A). The dual positive cells are considered as activated platelets and the percentage of the activated platelets were represented as bar graphs. At the end of 3^{rd} week, the percentage of activated platelets was significantly increased in the diabetes group (~32.4%) when compared to the control (~19.11%). We did not observe any significant changes in AMS

and aspirin-treated groups (Figure 2B). Similarly, at the end of the 10th week, the percentage of activated platelets increased significantly in the diabetes group (~47.19%) when compared to the control group (~35.24%). Moreover, both aspirin and AMS treatments significantly decreased this activation of platelets (~30.15 and 25.22% respectively) induced in diabetes.

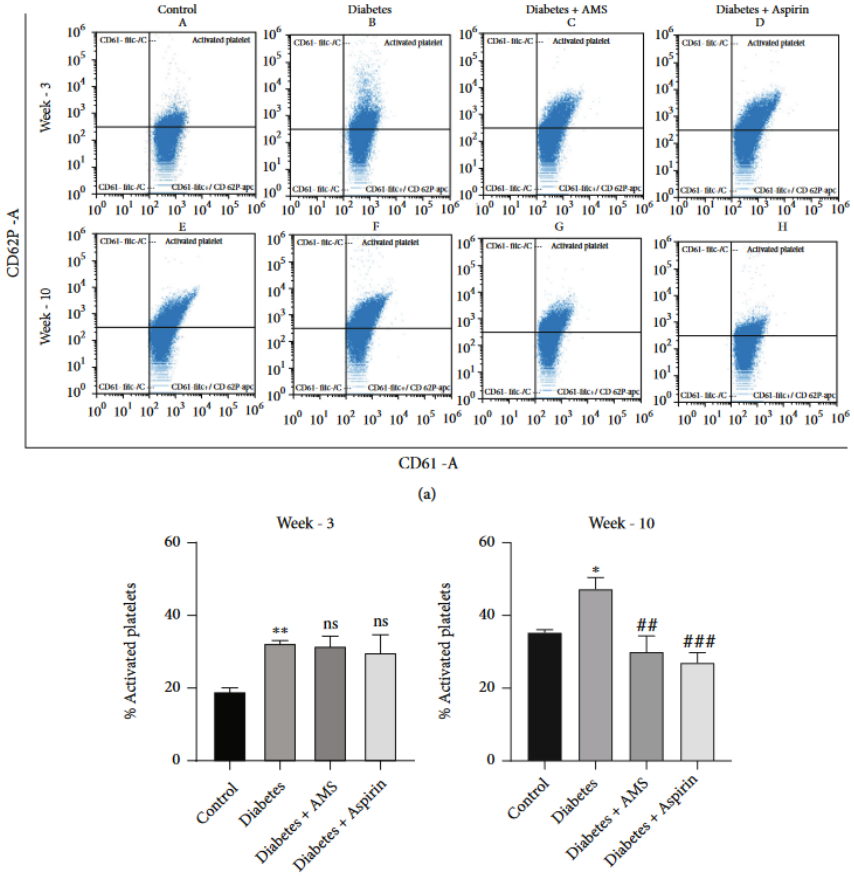

Figure 2: Flow-cytometry analysis of platelet activation showing percentage dual positive cells (CD61+, CD62P+). (A) Representation of the scattered plots of percentage platelet activation in (a, e), control (b, f), diabetic (c, g), AMS-treated diabetic (d, h), and aspirin-treated diabetic group after 3 and 10 weeks of study. Bar graph showing percentage platelet activation at the end of 3 weeks (B) and 10 weeks (C). All values are represented as mean ± SEM (N=4-5). *$p < 0.05$ vs control; **$p < 0.01$ vs control; ##$p < 0.01$ vs diabetes; ###$p < 0.001$ vs diabetes; ns=non-significant.

4.3. Effect of AMS on ADP-induced platelet aggregation

To assess the effect of AMS on platelet aggregation, flow cytometry analysis was performed on platelets derived from all the experiment groups in the absence or presence of ADP at the 3rd week and 10th week. Figure 3A shows FSC vs. SSC density plots of both with and without ADP-induced platelet aggregation where aggregates are gated as R2. In the absence of ADP, we did not observe any significant change in

the percentage of platelet aggregation in the diabetes group compared to control. However, a significant decrease (3-fold) in percent aggregation was observed in AMS- and aspirin-treated diabetes groups (Figure 3A and 3B). Similarly, as shown in Figures 3A and 3C, we observed a significant induction (~1.6-fold) in platelet aggregation by ADP in the diabetes group when compared to control. With AMS and aspirin treatment, we observed a significant decrease (~3.8 and 4.2-fold, respectively) in platelet aggregation when compared to the diabetes group.

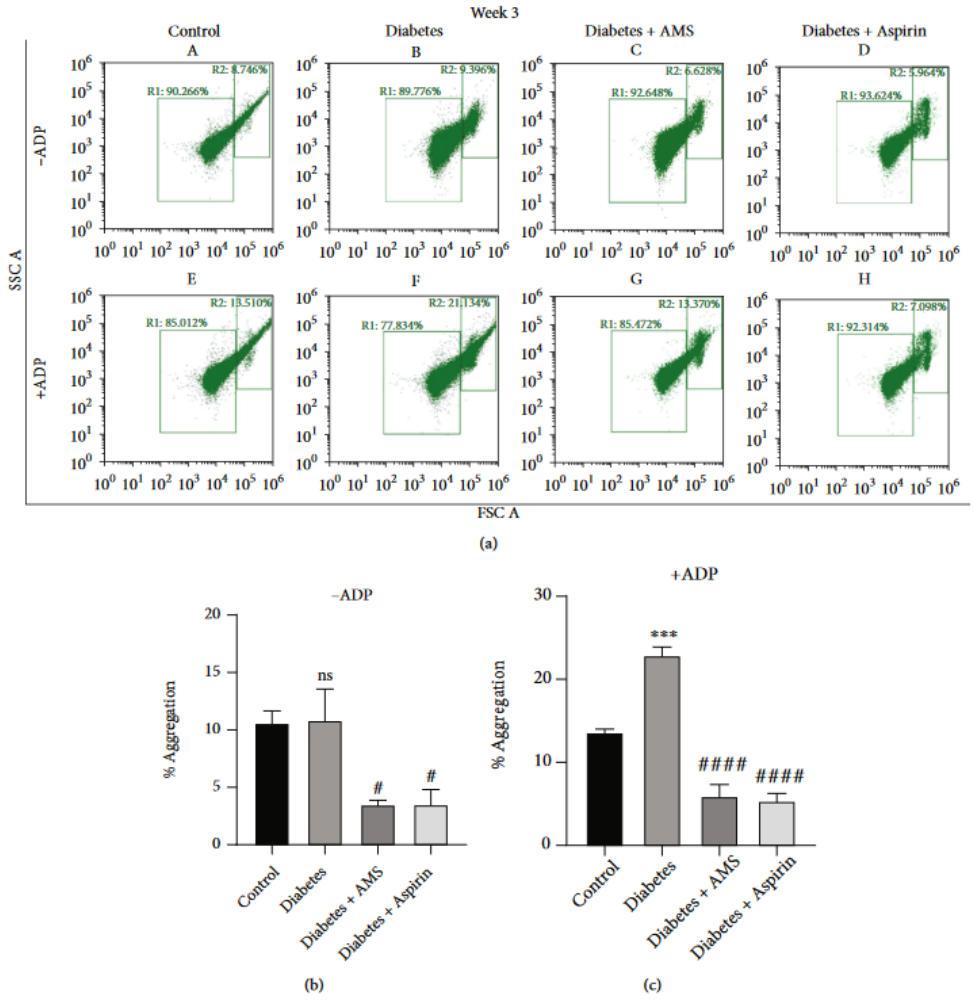

Figure 3: Flow-cytometry analysis of platelet aggregation after 3 weeks of treatment. (A) Scatter plot of forward vs. side scatter of platelets from control (a, e), diabetic (b, f), AMS treated diabetic (c, g), aspirin-treated diabetic (d, h), group representing the percentage of platelet aggregation in the absence and presence of ADP. The bar graph represents the percentage of platelet aggregation observed in the absence (B) and presence (C) of ADP. All values are represented as mean ± SEM (N=3). ***$p < 0.001$ vs control; $^{\#}p < 0.05$; $^{\#\#\#\#}p < 0.0001$ vs diabetes; ns=non-significant.

Similar flow cytometry analysis in the presence and absence of ADP was performed at the end of the 10th week and results were represented as FSC vs. SSC density plots (Figure 4A). In the absence of ADP, we observed that the percentage of platelet aggregation increased 1.2-fold in diabetic rats when compared to control (Figure 4B). A significant ($p<0.05$) decrease in the percentage of platelet aggregation was observed after AMS and aspirin treatment (~2.3 and 3.3-fold respectively). Similarly, ADP-induced aggregation was increased by 1.1-fold in diabetes and decreased by 1.1 and 1.5-fold in AMS and aspirin treatment groups (Figure 4C).

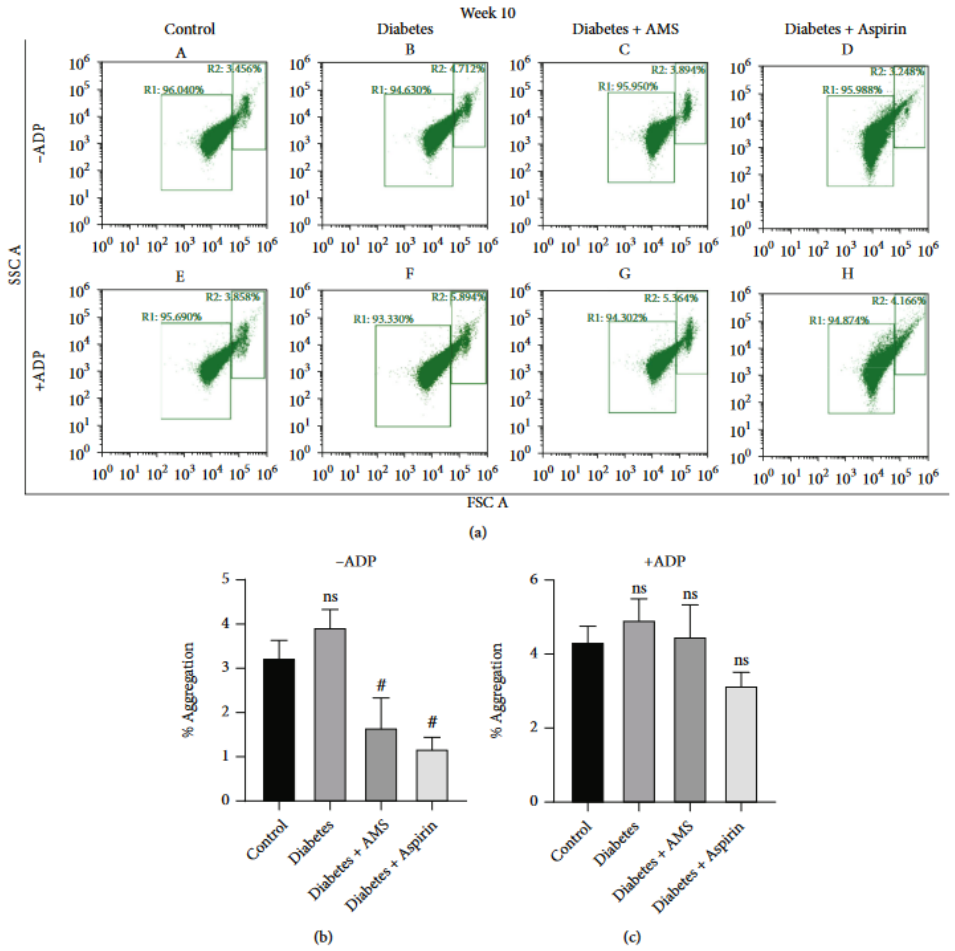

Figure 4: Flowcytometry analysis of platelet aggregation after 10 weeks of treatment. (A) Scatter plot of forward vs. side scatter of platelets from control (a, e), diabetic (b, f), AMS treated diabetic (c, g), aspirin-treated diabetic (d, h), group representing the percentage of platelet aggregation in absence and presence of ADP. The bar graph represents the percentage of platelet aggregation observed in the absence (B) and

presence (C) of ADP. All values are represented as mean ± SEM (N=3). $^{\#}p < 0.05$ vs diabetes; ns=non-significant.

4.4. Effect of AMS on diabetes-induced reactive oxygen species generation in platelets.

After the platelet activation and aggregation study, we measured the reactive oxygen species (ROS) levels in the platelets isolated from control, diabetic, and treated diabetic rats. ROS levels in platelets were measured by using 2', 7'-dihydro dichlorofluorescein diacetate (H_2DCFDA) dye and analyzed by flow cytometry. H_2DCFDA dye is a direct measure of the amount of ROS present in cells and the results are expressed as mean fluorescent intensity (MFI) of DCFDA. Platelet ROS levels were significantly ($p<0.05$) increased in the diabetic group when compared to the control. However, the ROS levels were decreased significantly ($p<0.05$) in platelets isolated from AMS-treated diabetic rats when compared to diabetes rats. We did not observe any change in ROS levels in platelets isolated from aspirin-treated diabetic rats.

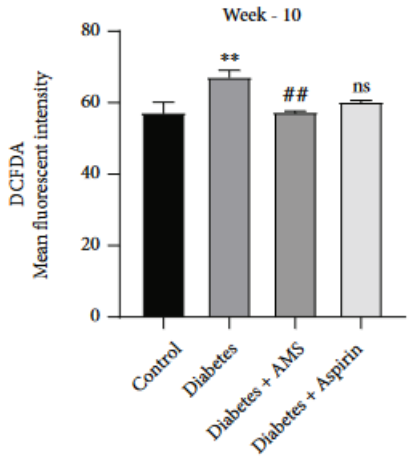

Figure 5: Comparison of ROS levels among control, diabetes, and treatment groups. All values are represented as mean ± SEM (N=3-4). ** $p < 0.01$ vs Control; $^{\#\#}p < 0.01$ vs diabetes; ns=non-significant.

4.5. Macrophage and platelet interaction by flowcytometry

Platelet macrophage interaction has been considered an important phenomenon for platelet activation in diabetes (53,54). To look at this interaction, macrophage and platelet were incubated together and FACS analysis was performed. THP 1, a well-known monocyte cell was differentiated with phorbol 12-myristate 13-acetate (PMA) and later cocultured with platelets collected from control, diabetes, and AMS/Aspirin-treated rats. The results are shown in the mean fluorescent intensity of CD61 positive cells (a marker of platelets) among CD14 positive THP1 macrophages. The data are represented as a bar graph (Figure 6). The increased mean fluorescent intensity was considered as aggregate cells of macrophages and platelets. In our data, a significant ($P < 0.05$) increase (~2.4-fold) in mean florescent

intensity was observed in platelets from the diabetes group when compared to the control. Although we observed a decrease in macrophage platelet interactions in the AMS and aspirin treatment groups (~1.2 and 1.5-fold) when compared to the diabetic group, these changes were not significant.

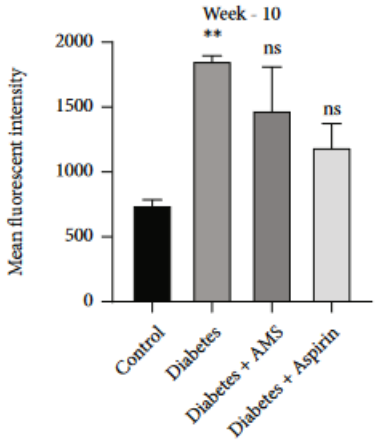

Figure 6: Macrophage platelet interaction in control, diabetes, and treatment groups. All values are represented as mean ± SEM (N= 3-5). ** $p < 0.01$ vs Control; ns=non-significant.

4.6. Measuring the altered metabolites of platelet by LCMS/MS metabolomics study

To evaluate the mechanism by which AMS is showing its beneficial effect in diabetes platelets, we performed a metabolomics study by LCMS/MS for control, diabetes, and diabetes treated with AMS rat platelets. PLS-DA plots show a clear separation between the groups (**Fig. 7A, B**). The significantly up-or downregulated metabolites were visualized in volcano Plots, binary comparisons of the levels of the 680 detected metabolites of platelets of control and diabetes were plotted by applying fold change (FC) (x-axis) and FDR-corrected p-values (y-axis) thresholds of 0.05 and 2/0.5, respectively, as shown in (**Fig.7C, D**). The volcano plots outlined the major metabolic differences. Further, we compared AMS-treated groups with the diabetes group to find out changes in the identified metabolites having differences in cellular metabolism. Compared to control, diabetes has 28 up regulated and 22 down regulated metabolites as in

diabetes vs AMS, 16 upregulated and 57 downregulated metabolites were found.

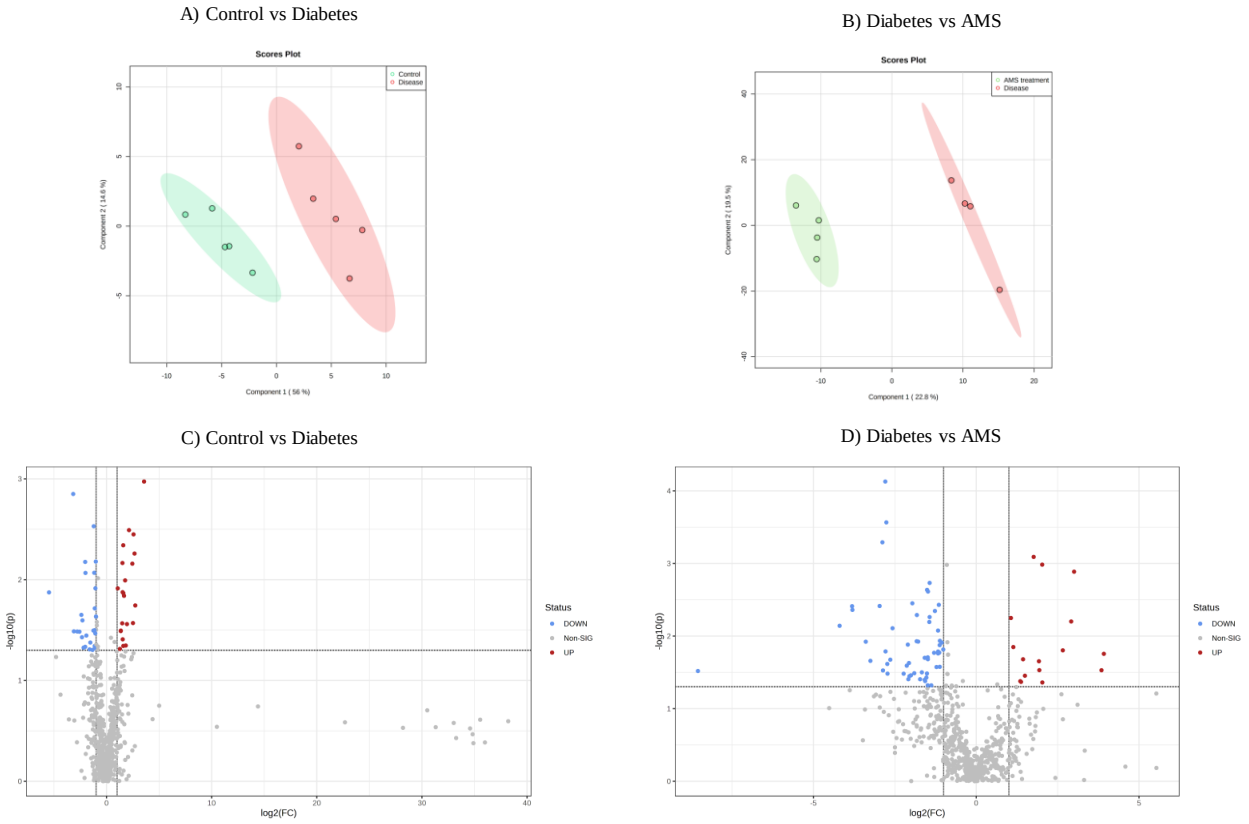

Figure 7: Identification of significantly altered metabolites. **[A, B]** PLS-DA plots of control in comparison to diabetes (Control vs. diabetes and diabetes in comparison with diabetes treated with AMS (Diabetes vs. Diabetes + AMS). **[C, D]** Volcano plots show significantly altered metabolites FDR-corrected p-values ($p<0.05$) (y-axis) and fold change (FC) (>2 or <0.5) (x-axis) of platelets of control in comparison with diabetes and diabetes in comparison with diabetes rat treated with AMS respectively.

Further, a heatmap showing the cluster differentiation of significantly altered metabolites of control vs. diabetes and diabetes vs. diabetes + AMS groups (**Fig. 8A, B**). Further pathway analysis of the significantly differential metabolites reveals the arachidonic acid pathway as a majorly altered pathway in diabetes compared to control (**Fig. 9 A, B**). Among the differential metabolites of the arachidonic acid pathway, 5 metabolites showed a significant change among three groups i.e. common in control vs. diabetes and diabetes vs. diabetes + AMS (**Table 2**). These metabolites include 13,14-dihydro-15-keto Prostaglandin F2alpha, 7-hydroxy docosahexaenoic acid, Prostaglandin E2 and 15-HETE are downregulated in diabetes and upregulated after AMS treatment except for Prostaglandin E2. Further 15 keto prostaglandins A1 is

upregulated in diabetes compared to control. After AMS treatment there is a much higher fold change upregulation than diabetes.

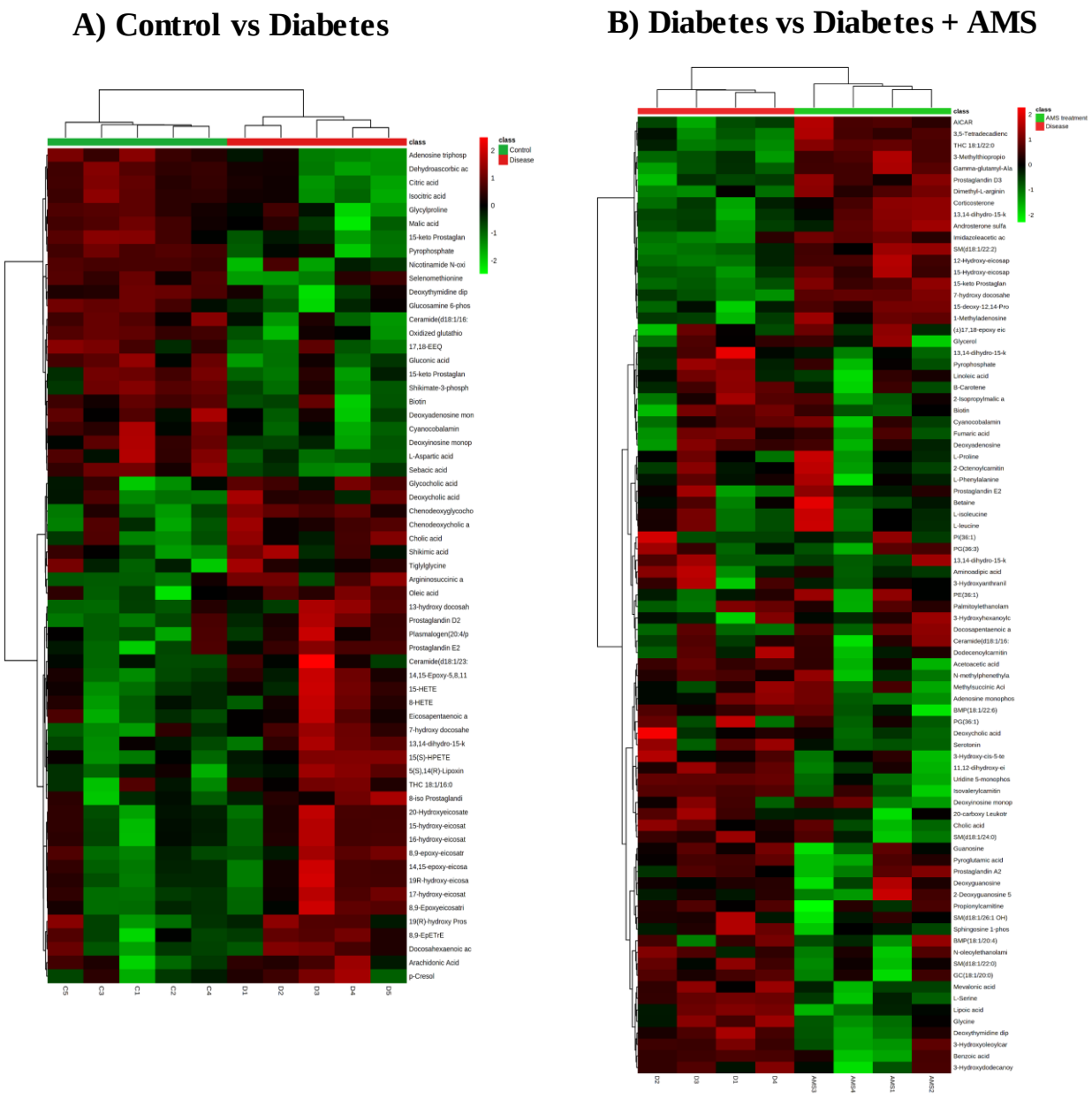

Figure 8: Heat map showing cluster differentiation of significant metabolites. **[A]** Heat map of control in comparison to diabetes (Control vs Diabetes). **[B]** Heat map of diabetes in comparison to diabetes rats treated with AMS (Diabetes vs Diabetes + AMS).

Table 2: Differentially expressed metabolites of arachidonic acid pathway in platelets

	Metabolites	Control vs Diabetes		Diabetes vs AMS	
		Fold change	P value	Fold change	P value
	Arachidonic acid metabolism				
1	13,14-dihydro-15-keto Prostaglandin F2alpha	0.19725	0.047276	9.485343	0.017562
2	15-keto Prostaglandin A1	6.511997	0.026944	73.45557	0.000812
3	7-hydroxy docosahexaenoic acid	0.080655	0.006665	60.40935	0.001038
4	Prostaglandin E2	0.132008	0.019253	0.085757	0.012166
5	15-HETE	0.090741	0.008541	18.47625	0.005638

A) Control vs Diabetes

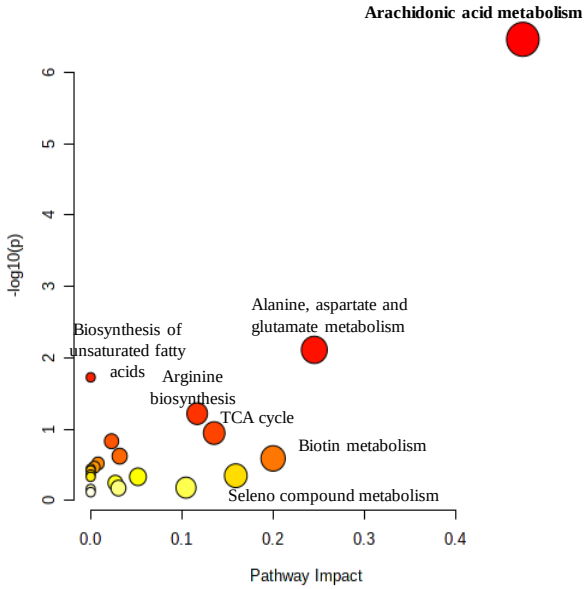

B) Diabètes vs Diabetes + AMS

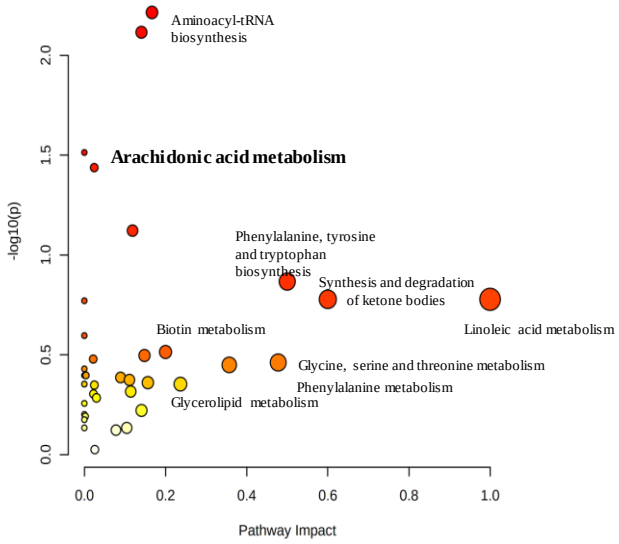

Figure 9: Pathway analysis of significant metabolites. **[A]** Pathway analysis plot of control in comparison to diabetes (Control vs. Diabetes). **[B]** Pathway analysis plot diabetes in comparison to diabetes rats treated with AMS (Diabetes vs Diabetes + AMS)

OBJECTIVE 2- Finding the therapeutic efficacy of paricalcitol, a vitamin D analog in a rat model of NAFLD.

4.7. Body weight and food intake changes in rats

The body weight of rats was monitored every week till the end of the study (20 weeks). The percentage changes in body weight of rats were calculated and the graph was plotted (**Fig. 10A**). There was a significant increase in the percentage body weight change of NAFLD rats starting from the11th week to the 20th week (except week 12) of the study period compared to control. However, NAFLD rats treated with paricalcitol showed no changes in percentage body weight change compared to NAFLD rats. Similarly, rats were also monitored for food intake where both NAFLD and NAFLD treated with paricalcitol (NAFLD + PCAL) rats showed less food intake compared to control (**Fig. 10B)**.

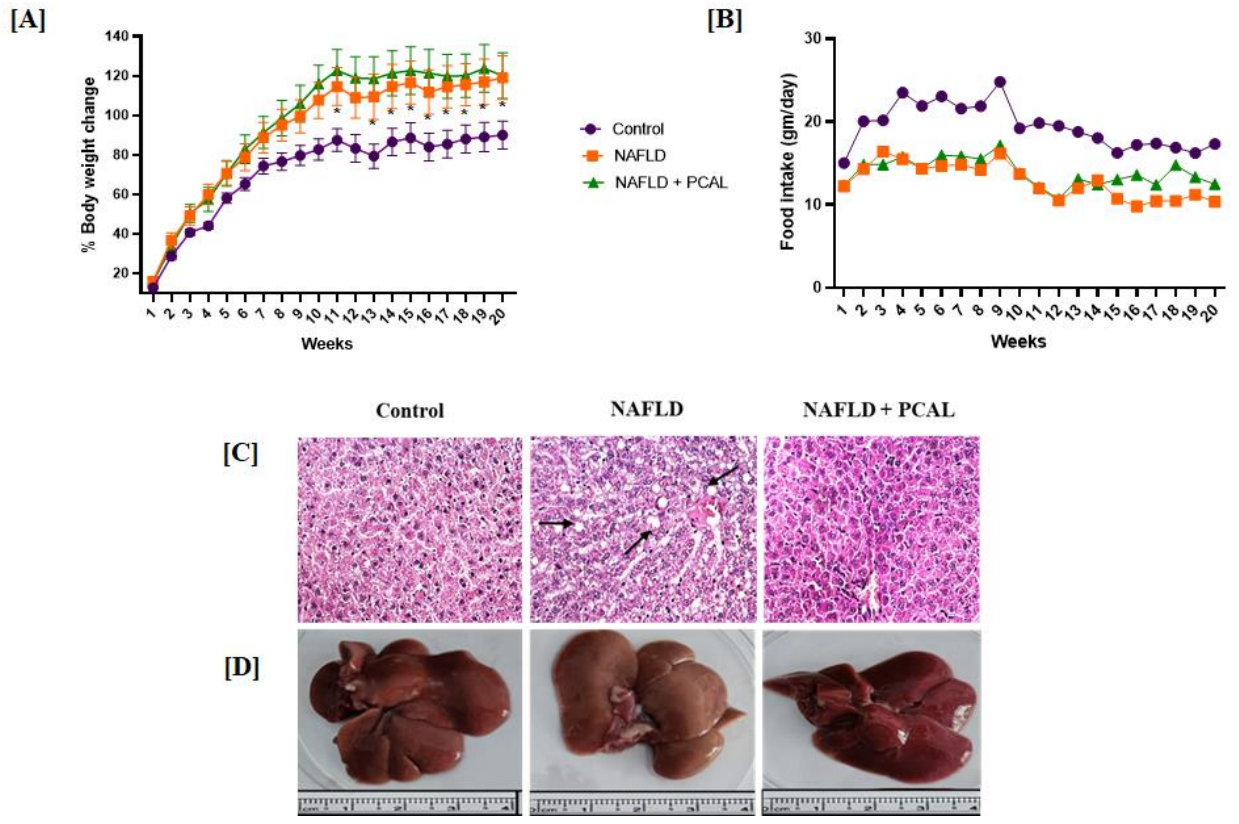

Figure 10. Rats were fed with a CDHF diet for 20 weeks and treated with paricalcitol. **[A]** Percentage (%) body weight changes, **[B]** changes in food intake, and **[C, D]** liver histopathology and morphological images of control, NAFLD and NAFLD + PCAL groups. The data were analyzed using a two-way ANOVA followed by Tukey's test and represented as mean ± SEM. *$p < 0.05$ (n=7).

4.8. Paricalcitol reduced the histopathological changes in NAFLD rat liver

The liver of rats was collected after euthanizing the animals during the 20th week of the study (**Fig. 1D**). Liver morphology of NAFLD is slightly varied by color compared to control rats whereas treatment with paricalcitol improved the morphology in NAFLD liver to normal. Further, histopathological evaluation of rat liver by H&E-stained sections showed fat accumulation, ballooning, and inflammation in NAFLD rats compared to the control. After paricalcitol treatment (NAFLD + PCAL group), normalization of these parameters was observed when compared to NAFLD liver (**Fig. 1C**).

4.9. Effect of paricalcitol on serum biochemical parameters

The effect of paricalcitol on serum biochemical parameters was measured and the changes were ploted as bar graphs (**Fig. 11**). Serum levels of uric acid, AST, ALT, and insulin were significantly increased in NAFLD compared to control. Paricalcitol treatment effectively reduced the levels of AST, ALT, and insulin but not uric acid in the NAFLD + PCAL group. Moreover, serum lipid parameters such as LDL and triglyceride were significantly elevated in serum of NAFLD compared to control. Paricalcitol significantly reduced LDL and triglyceride in the NAFLD + PCAL group. Further, HDL levels were reduced in NAFLD and elevated significantly after paricalcitol treatment. There was no significant change observed in cholesterol levels among all the groups.

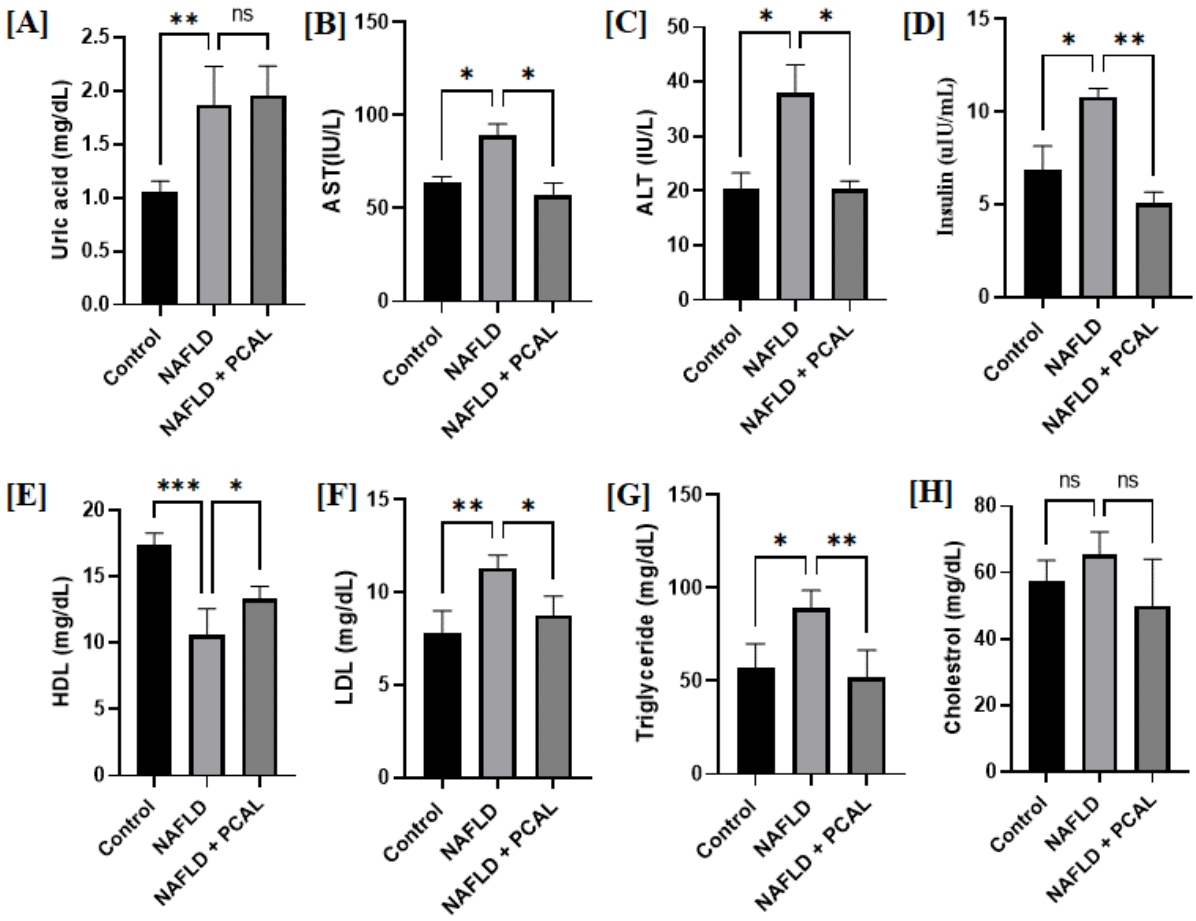

Figure 11. Bar graphs showing changes in various serum biochemical parameters of control, NAFLD and NAFLD + PCAL groups where **[A]** uric acid**, [B]** AST, **[C]** ALT, **[D]** insulin, **[E]** HDL, **[F]** LDL, **[G]** triglyceride and **[H]** cholesterol. The data were analyzed using a One-way ANOVA followed by Tukey's test and represented as mean ± SEM. *p< 0.05, **p< 0.01, ***p<0.001 (n=3-4 from two independent blots).

4.10. Effect of Paricalcitol on the reversal of protein acetylation in the liver of NAFLD rats.

Protein acetylation was measured in the liver by western blot (**Fig. 12A, D**). There was an increase in acetylated lysin protein in the liver of NAFLD rats compared to the control. Interestingly, paricalcitol reversed the acetylation status in NAFLD + PCAL liver. Further, the protein expression of deacetylating enzymes such as SIRT3 (**Fig. 12B, E)** and SIRT1 was measured **(Fig. 12C, F**) where NAFLD liver showed a significant decrease in expression of both SIRT1 and SIRT3 in NAFLD compared to control. Paricalcitol treatment has significantly improved the SIRT1 and SIRT3 levels in the NAFLD + PCAL group.

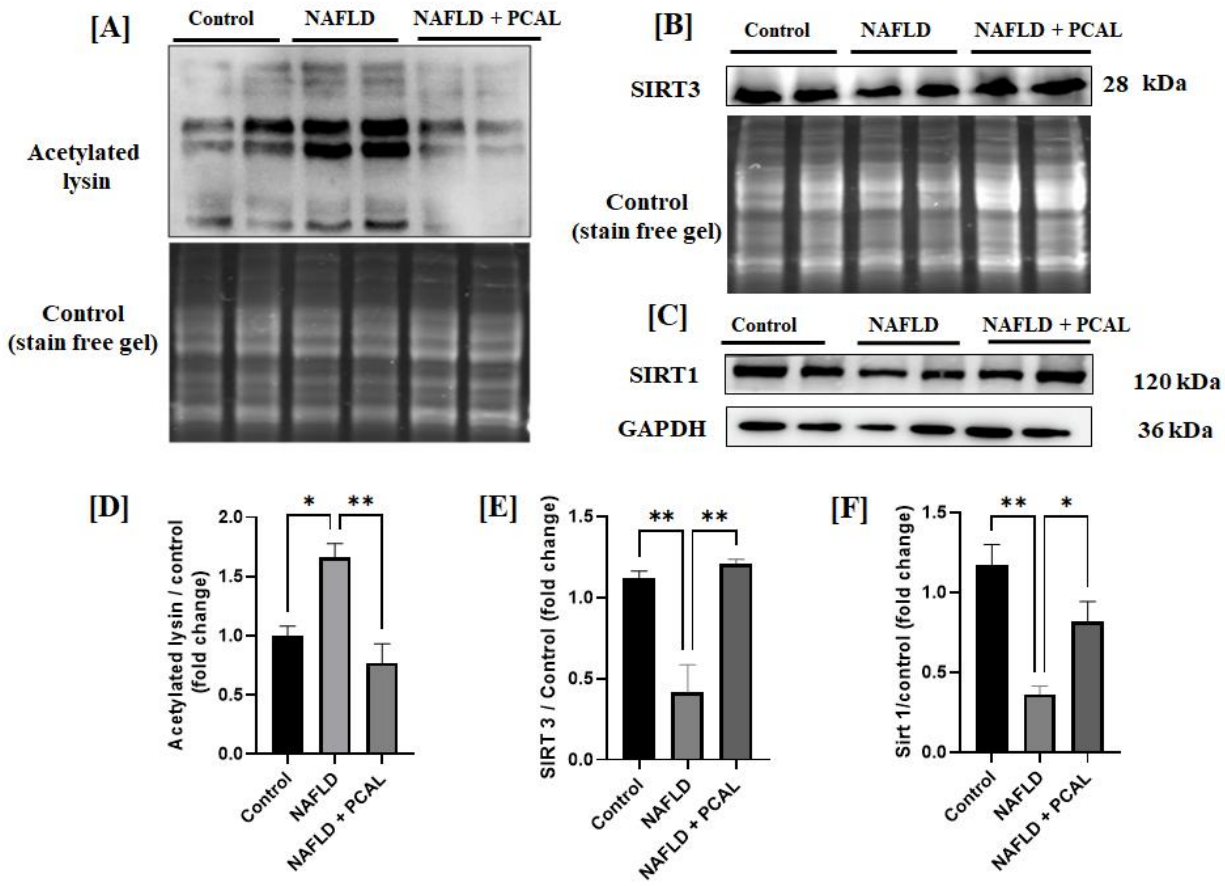

Figure 12. The acetylation status of protein was measured in rat liver of control, NAFLD, NAFLD + PCAL groups. **[A, D]** Total acetylated lysin expression**. [B, E]** Protein expression of SIRT3 and **[C, F]** Protein expression of SIRT1. The data were analyzed using a One-way ANOVA followed by Tukey's test and represented as mean ± SEM. *p< 0.05, **p< 0.01 (n=3-4 from two independent blots).

4.11. Paricalcitol regulates the inflammation in the liver of NAFLD rats by attenuating the acetylation of NFκB and modulating gene expression of inflammatory makers.

We measured the levels of the transcription factor NFκB in the liver of control, NAFLD, and paricalcitol (NAFLD + PCAL) groups by western blot (**Fig. 13A-C**). Data showed a significant increase in the expression of the NFκB in the NAFLD compared to the control. Similarly, we checked the expression of the acetylated NFκB. Data showed a significant increase in the levels of the acetylated NFκB in NAFLD compared to the control. After paricalcitol treatment (NAFLD + PCAL group), a significant decrease was seen in both total and acetylated NFκB expression. Further, mRNA expression of inflammatory genes such as TNFα, IL 1ß, and NFκB was measured by PCR (**Fig. 13E-H**). Data showed a significant increase in expression of TNFα, IL 1ß, and NFκB in rat liver of NAFLD when compared to control. Further paricalcitol treatment has significantly reduced this gene expression in the NAFLD + PCAL group. Additionally, the

inflammation in the liver was measured by MPO assay, where the data showed an increase (but not significant) in MPO activity in NAFLD the rat liver compared to control (**Fig. 13D**). But paricalcitol treatment showed a significant reduction in MPO activity in NAFLD + PCAL liver.

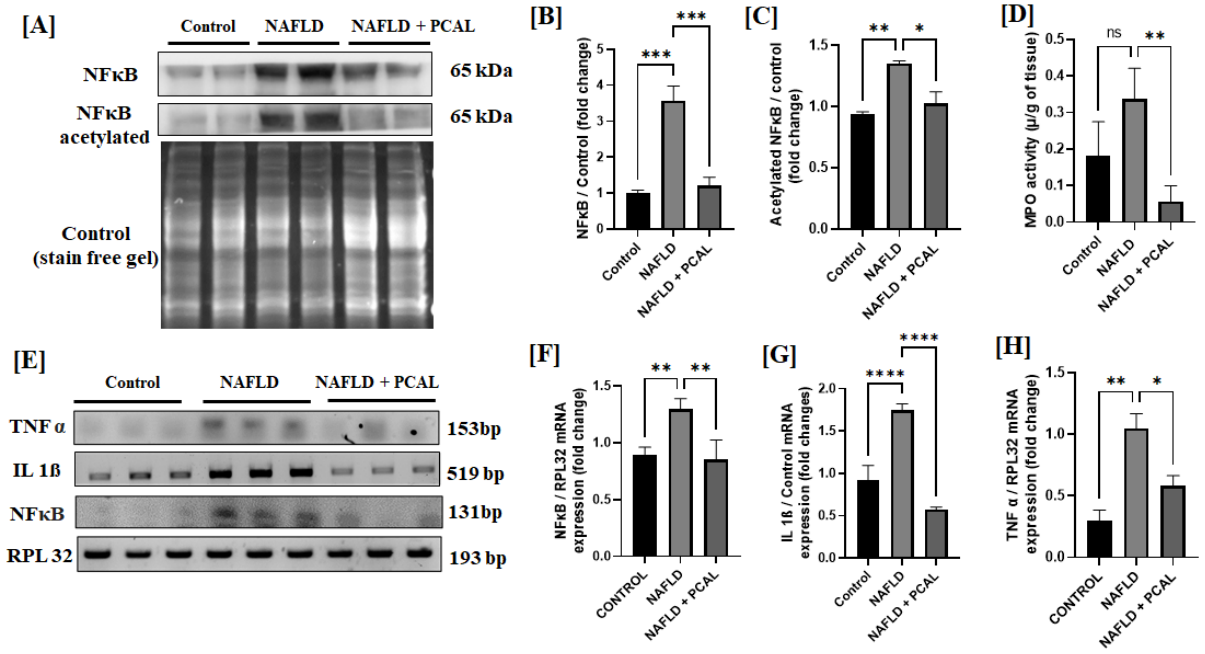

Figure 13: Expression of inflammatory markers in the liver of control, NAFLD, NAFLD + PCAL group. **[A-C]** protein expression of NFκB & acetylated NFκB expression in the rat liver, **[D]** MPO activity, **[E-H]** mRNA expression of TNFα, IL 1ß, and NFκB. The data were analyzed using an ordinary one-way ANOVA and represented as mean ± SEM. *p< 0.05, **p< 0.01, ***p<0.001, ****p<0.0001 (n=4 from two independent blots).

4.12. Paricalcitol attenuates the acetylation of FoXO3A and gene expression of oxidative stress markers in the liver of NAFLD rats.

We measured the protein levels of the transcription factor FOXO3A in the liver of control, NAFLD, and paricalcitol (NAFLD + PCAL) groups by western blot (**Fig. 141A-C**). Data showed a significant increase in the expression of FOXO3A in the NAFLD compared to the control. Similarly, the liver after paricalcitol treatment (NAFLD + PCAL group) showed a significant decrease in the expression of FOXO3A. Further, we check the levels of the acetylated FOXO3A. Data showed a significant increase in the levels of the acetylated FOXO3A in NAFLD compared to the control. However, the paricalcitol treatment showed a significant decrease in the levels of acetylated FOXO3A**.** Then we measured oxidative stress parameters in the rat liver by evaluating mRNA gene expression levels of two antioxidant genes, MnSOD and catalase (**Fig. 14D-F**). Data showed a significant decrease in the expression of the MnSOD and catalase genes in

the NAFLD compared to the control. The paricalcitol treatment showed a significant increase in the expression of both MnSOD and catalase genes in the NAFLD + PCAL group when compared to the NAFLD group.

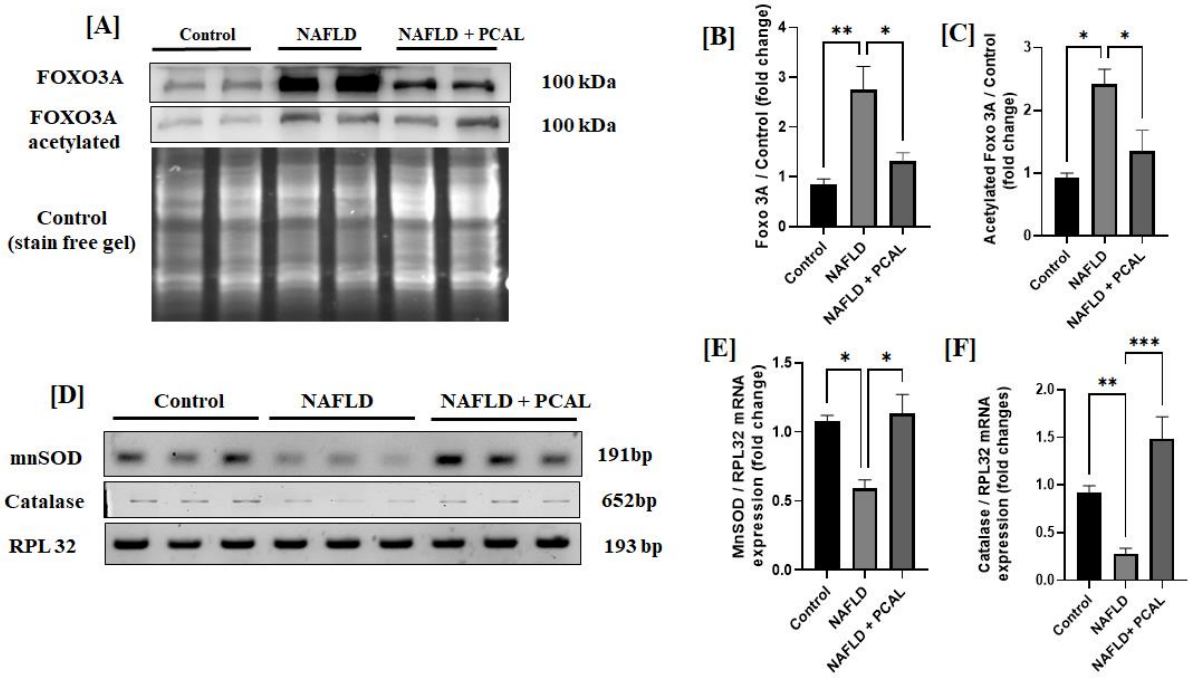

Figure 14: Expression of oxidative stress markers in the liver of control, NAFLD, NAFLD + PCAL groups. **[A-C]** FOXO3A and its acetylated protein status; **[D-F]** mRNA expression of MnSOD and catalase. The data were analyzed using a One-way ANOVA followed by Tukey's test and represented as mean ± SEM. *p< 0.05, **p< 0.01, ***p<0.001 (n=3-4 from two independent blots).

4.13. Paricalcitol attenuates oxidative stress and enhances the antioxidant activity in the liver of NAFLD rats.

We measured the oxidative stress in the liver of Control, NAFLD, and Paricalcitol (NAFLD + PCAL) groups using a lipid peroxidation assay. Our data showed that lipid peroxidation was significantly increased in the liver of NAFLD rats compared to the control rats. Paricalcitol treatment significantly decreased lipid peroxidation levels in NAFLD + PCAL rats. (**Fig. 15A)**. Additionally, we measured ROS levels by using a fluorescence dye, DCFDA in the liver homogenate of control, NAFLD, and Paricalcitol (NAFLD + PCAL) groups. Our data showed that the ROS level increased significantly in the NAFLD group compared to the control. The Paricalcitol treatment showed a significant decrease in the ROS levels in the liver of NAFLD + PCAL rats (**Fig. 15B**).

Furthermore, to evaluate the antioxidant properties we measured GSH levels, an antioxidant in the liver of control, NAFLD, and paricalcitol (NAFLD + PCAL) groups. Data showed that the GSH levels in the liver were decreased in NAFLD rats compared to the control. However, paricalcitol treatment significantly increased GSH levels in the NAFLD + PACL group (**Fig. 15C**). Further, catalase, an antioxidant enzyme, activity in the liver of control, NAFLD, and paricalcitol (NAFLD + PCAL) groups were measured. Our data showed that the catalase enzyme activity was significantly decreased in the NAFLD liver compared to the control. However, paricalcitol treatment showed a significant increase in catalase enzyme activity in the liver of NAFLD + PCAL rats (**Fig. 15D**). We have also measured the percentage of total antioxidant levels in the liver of control, NAFLD, and Paricalcitol (NAFLD + PCAL) groups by using DPPH assay. Our data showed that the total antioxidant activity was significantly decreased in the NAFLD liver compared to the control. Paricalcitol treatment significantly increased the percentage of total antioxidant activity in the liver of NAFLD + PCAL rats (**Fig. 15E**).

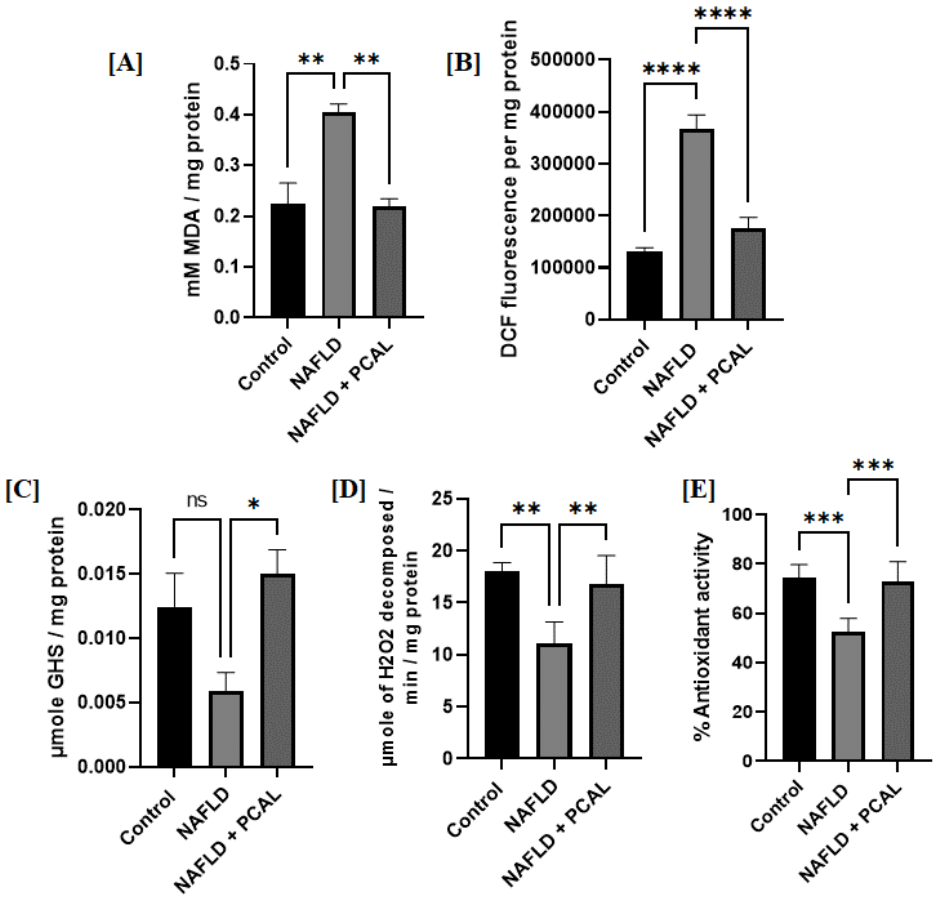

Figure 15: Oxidative stress and antioxidant level/activity were measured in the liver of control, NAFLD, NAFLD + PCAL groups. **[A]** Lipid peroxidase activity; **[B]** ROS level; **[C]** GSH concentration; **[D]**

Catalase activity; **[E]** % Total antioxidant activity. The data were analyzed using a One-way ANOVA followed by Tukey's test and represented as mean ± SEM. *p< 0.05, **p< 0.01, ***p<0.001, ****p<0.0001 (n=3-4).

4.14. Effect of paricalcitol on cardiac function measured by echocardiography analysis.

The heart weight of control, NAFLD and NAFLD + PCAL groups were measured and neutralize with tail length. There was an increase in heart weight by tail length ration in NAFLD group at 20th week of CDHF induced NAFLD. After paricalcitol treatment, there was a decrease in heart weight by tail length ration in NAFLD+ PCAL group (**Fig. 16**). To see the effect of paricalcitol on cardiac function, we performed the echocardiography of all the rats during the 12^{th} $16^{th,}$ and 20^{th} week of the CDHF-induced NAFLD. In the 12^{th} week there were no significant changes observed in the echocardiography parameters among all the groups (**Fig. 17**).

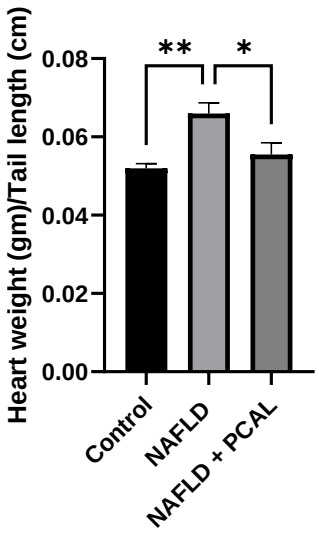

Figure 16: Changes in heart weight among control, NAFLD and NAFLD treated with paricalcitol (NAFLD + PCAL). Results are represented as mean ± SME, N=4, *p<0.05, **p<0.01,

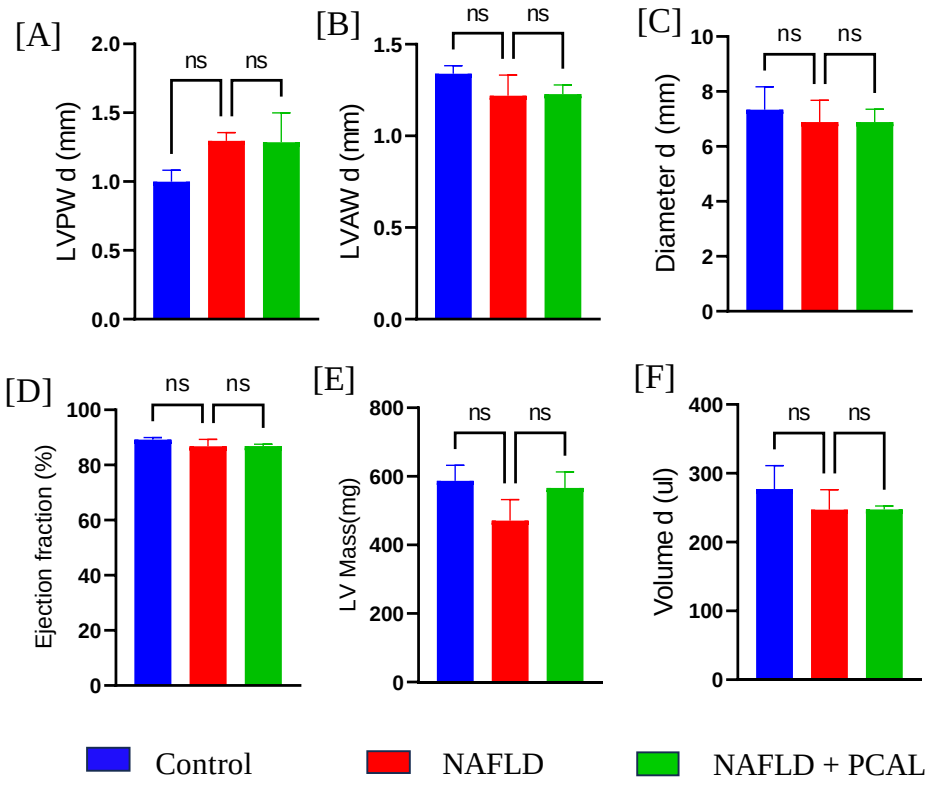

Figure 17: Echocardiographic changes in control, NAFLD and NAFLD treated with paricalcitol (NAFLD + PCAL) at 12th week of study. **[A]** Left ventricular posterior wall thickness diastole (LVPW d), **[B]** left ventricular anterior wall thickness diastole (LVAW d), **[C]** diameter diastole, **[D]** ejection fraction, **[E]** left ventricular (LV) mass, **[F]** volume diastole. Results are represented as mean ± SME, N=3-4, ns= non-significant.

In the 16 weeks there was a significant increase in the anterior and posterior wall thickness of diastole (**Fig. 18**). Further there is a decreased diastolic volume and diameter in NAFLD. The ejection fraction was also decreased in disease condition vs. control. All these parameters have been reversed after paricalcitol treatment in the 16th week.

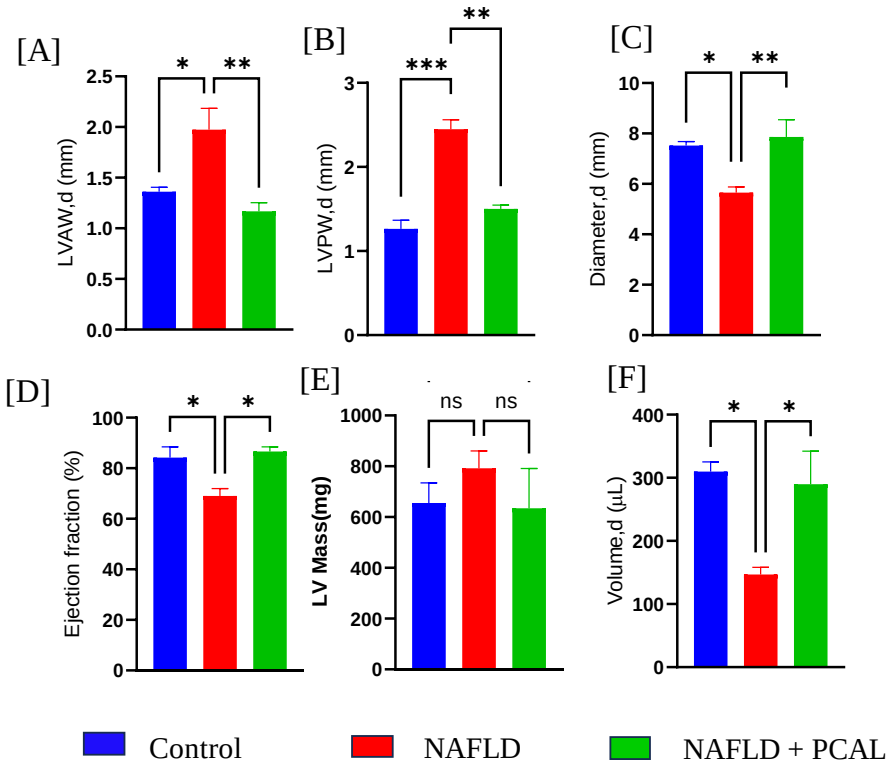

Figure 18: Echocardiographic changes in control, NAFLD and NAFLD treated with paricalcitol (NAFLD + PCAL) at 16th week of study. **[A]** Left ventricular posterior wall thickness diastole (LVPW d), **[B]** left ventricular anterior wall thickness diastole (LVAW d), **[C]** diameter diastole, **[D]** ejection fraction, **[E]** left ventricular (LV) mass, **[F]** volume diastole. Results are represented as mean ± SME, N=3-4, *p<0.05, **p<0.01, ***p<0.001.

Similarly, at the 20th week of CDHF-induced NAFLD, there is an elevated diastolic anterior and posterior wall thickness, LV mass, and diastolic diameter in NAFLD (**Fig. 19**). Ejection fraction has been found to be significantly decreased in NAFLD. After paricalcitol treatment, all these parameters have been reversed effectively except for diastolic diameter.

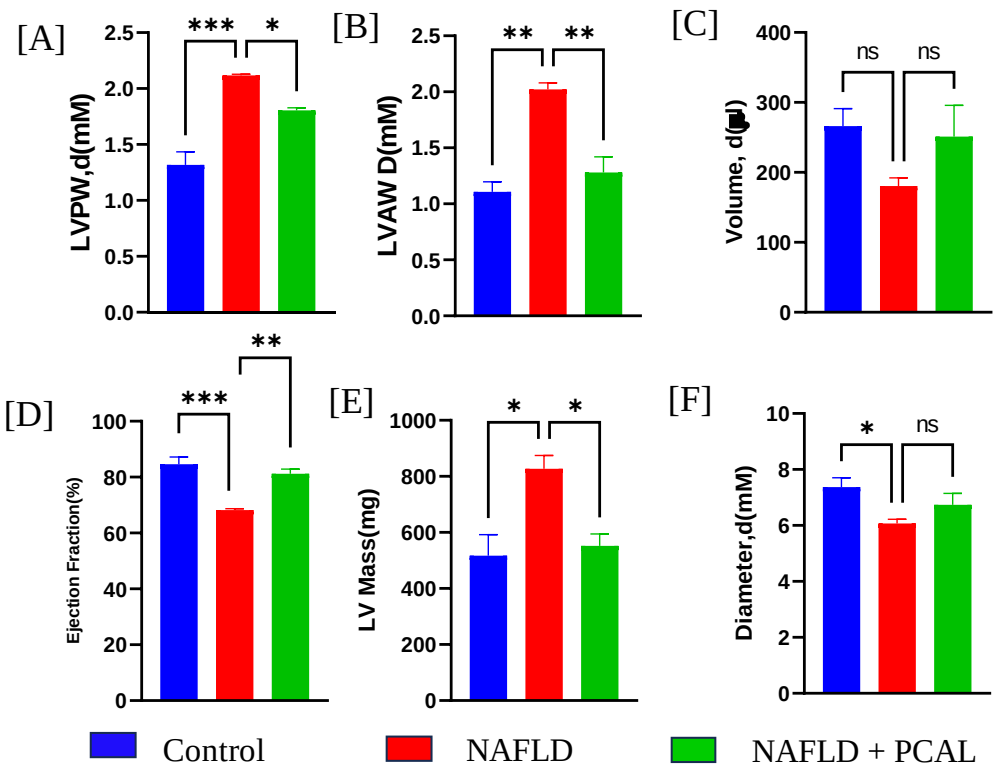

Figure 19: Echocardiographic changes in control, NAFLD and NAFLD treated with paricalcitol (NAFLD + PCAL) at 20th week of study. **[A]** Left ventricular posterior wall thickness diastole (LVPW d), **[B]** left ventricular anterior wall thickness diastole (LVAW d), **[C]** diameter diastole, **[D]** ejection fraction, **[E]** left ventricular (LV) mass, **[F]** volume diastole. Results are represented as mean ± SME, N=3-4, *p<0.05, **p<0.01, ***p<0.001.

5. Discussion

Nonalcoholic fatty liver disease (NAFLD) and diabetes mellitus (DM) are often co-existing conditions. Both have been viewed as a sign of metabolic syndrome (55,56). Additionally, both have been linked to an elevated risk of cardiovascular disease (CVD), pointing diabetes and NAFLD as cardiometabolic illnesses (57). The study showed that patients with diabetes and NAFLD had a doubled risk of CVD compared with patients with diabetes but without NAFLD. The data point towards an additional effect of NAFLD in patients with diabetes in long-term risk of cardiovascular disease (CVD). Therefore, the presence of diabetes and NAFLD makes the cardiometabolic disease more complex and are major obstacles to find effective therapy to reduce cardiovascular complications (58,59). To achieve this goal, we need to have a thorough mechanistic understanding of the disease pathogenesis and cellular signaling pathways that contribute to CVD (59). We are exploring natural compound and FDA-approved drugs for the therapeutic intervention of cardiometabolic diseases. In the current study, we investigated the effect of Allyl methyl sulfide (AMS), a metabolite of garlic, on platelet activation in diabetes and measured the direct beneficial effect in CVD. Further, we tried to repurpose paricalcitol, an FDA-approved medication for chronic kidney disease, on NAFLD and associated CVD.

Previous scientific literature identified numerous risk factors i.e., hyperglycemia (60–62), dyslipidemia (63,64), inflammation (65,66), endothelial dysfunction, and oxidative stress (67,68), which together can induce complexity including cardiovascular complications in diabetes. Studies have also identified that alteration of normal platelet function as one of the major risk factors of diabetic complication and characterized by increased thromboxane synthesis (69), reduced membrane fluidity (70), and increased expression of activation-dependent adhesion molecules (e.g., GpIIb-IIIa, P-selectin) (71). All of these changes make platelets more reactive and create a prothrombic environment in diabetes patients (72,73). Although there are many studies supporting the use of antiplatelet drugs such as aspirin and clopidogrel in diabetic cardiovascular complications, it has been ineffective because of its adverse reactions. Further, the studies focusing on platelet dysfunction in diabetes and its modulation by pharmacological agents, are limited.

Recent literature says that among all the popular natural remedies, organosulfur compounds from garlic have shown a potential antidiabetic and as well as antithrombotic effect in diabetic individuals (74–78). Previous research work also supported the role of garlic to attenuate cardiovascular complications in diabetes (75). Allyl methyl sulfide (AMS) is one of the important sulfur compounds obtained from garlic and studies showed that AMS is a major metabolite that is detected in the human breath and plasma (79). Our previous study on AMS suggested that chronic administration of AMS is safe in control rats, where the body weight, food, and water intake along with the histopathology of major organs and serum biomarkers

remained normal (23). Further, the same study showed a beneficial effect of AMS on isoproterenol-induced cardiac fibrosis and dysregulated extracellular matrix (ECM) deposition in the myocardium (23). Also, our recent finding showed a cardio-protective effect of AMS in pressure overload-induced cardiac hypertrophy and heart failure by ameliorating endogenous antioxidants and mitochondrial function (39). Further research identified the therapeutic role of AMS on type 1 diabetes where different parameters like blood glucose, HbA1c, oxidative stress, inflammation, and insulinotropic activity were normalized after AMS treatment, All the above parameters remained normal in control rats after AMS administration (80,81). However, there is no study to find the effect of AMS on platelet activation. To see this, in the present study, we developed an STZ-induced animal model of diabetes and treated it with AMS. In diabetes, controlling hyperglycemia is the primary goal to reduce complications in diabetes. Poor glycaemic control affects platelet activation and vascular dysfunction in diabetes (82). Therefore, primarily we tried to see the effect of AMS on glucose levels where AMS administration to rats reduced blood glucose levels. Further, the result showed that AMS is more effective in reducing blood glucose levels in diabetic rats than aspirin. Our data supports the recent studies on AMS, where AMS administered to STZ-induced diabetic rats showed a significant decrease in blood glucose levels (81,83).

Hyperglycemia along with other factors helps to aggregate the platelets in the presence of a small stimulus. Such platelets are referred to as hyperactivated platelets (84). This hyper-activated platelet has distinct morphology and expresses P-selectin (CD69P) and GP IIb/IIIa receptors on the surface(85–87). Supporting the previous data, our present study also observed an increase in platelet activation (CD62P levels) in type 1 diabetic rats when compared to non-diabetic rats. This activation of platelets was higher at a later stage (10 weeks) when compared to the initial stage (3 weeks) of diabetes. Moreover, we also observed the effect of AMS on platelet activation. Interestingly, we found a little reduction in platelet activation after initial treatment for 3 weeks with AMS but a significant decrease was found after 10 weeks of treatment. Here our data suggest that long-term administration of AMS has a superior effect on the reduction of platelet activation in diabetes.

Increased platelet activation results in increased platelet aggregation and has been detected in diabetes mellitus (53,54). This increased platelet aggregation is a result of increased systemic production of TxA 2 by platelet (88), increased sensitivity of platelet agonists like ADP (89), and impaired production of platelet aggregation inhibitors PGI 2 and NO (90,91). The previous finding has shown that the platelet of the diabetes patient was found to be 1.6-fold more sensitive to ADP-induced aggregation than that of non-diabetes persons (92). In the present study, we observed the aggregation of platelets (basal level) and their sensitivity to ADP stimuli in both the early and late stages of diabetes. At the early stages of the disease, there was no difference in baseline aggregation property of platelets between diabetes and control groups.

However, in the presence of ADP, the diabetic platelets showed an increase in aggregation than the control group. The data suggests that the platelets from diabetic rats were highly sensitive and prone to develop thrombus formation. A decrease in baseline aggregation was observed in diabetic rats after AMS and aspirin treatment. The percentage of aggregation was further reduced when the platelets were activated by the addition of ADP. The study suggests that AMS has a beneficial effect in reducing platelet sensitivity and aggregatory properties. Similar to platelet aggregation data in week 3, we observed a decrease in baseline platelet aggregation after AMS and aspirin treatment. Interestingly, in the 10th week of diabetes, we did not observe any increase in ADP-induced platelet aggregation in the diabetes group when compared to control. Although we cannot explain the reason for not showing the sensitivity of platelets after ADP addition at week 10, it may be due to desensitization of P2Y1 and P2Y12 ADP receptors of platelets after the long-term interaction with endogenous ADP in chronic diabetes (93). Further, the control group in 10th week showed higher basal platelet aggregation than control group at 3rd week. This can be explain by the fact that age itself may enhanced the platelet aggregation in absence of diabetes (94). After treatment with AMS for 10 weeks, we observed a decrease in aggregation. The data overall indicated that inhibition was less at later stages of diabetes and may be due to the alteration of platelet structure and expression of major protein levels that resist the AMS's beneficial effect.

Next, we correlated the platelet aggregation phenotype with intracellular ROS production. Increased ROS has been observed in activated platelets and activates the PKC pathway which led to platelet hyperactivity and aggregation (95). Supporting the previous literature, our study also found increased ROS content in diabetic platelets when compared to control. A recent study on AMS showed the effect of oxidative stress on diabetes. AMS administration improved oxidative stress in STZ-induced hyperglycemic rats (81). Based on their observation, we evaluated the endogenous ROS generation in platelets after AMS treatment and found an inhibitory effect of AMS on ROS production in platelets.

Increased ROS production can activate the platelets and help to participate in the signaling event of atherosclerosis in diabetes by forming aggregates with monocytes through P-selectin–PSGL-1 interactions (96). Thereby platelets play an important role in promoting inflammation in diabetes. The inflammatory condition created by PSGL–1–1-mediated monocyte activation leads to the synthesis and release of various chemokines, cytokines, and reactive oxygen species. Monocyte platelet interactions also have a role in the coagulation system by surface expression of phosphatidylserine (97). Previous literature suggested that increased platelet-monocyte aggregates are the indicator of *in vivo* platelet activation. These aggregates are responsible for the prothrombic stage and play a major role in the development of atherosclerosis in type 1 diabetes (98,99). Additionally, macrophage accumulation also plays a vital role in causing diabetic complications (100). It was reported that a similar interaction between macrophages and platelets causes

releases of chemokines and phagocytosis of platelets which further involved in atherothrombosis formation (101,102). In the present study, we observed platelet macrophage interactions to evaluate the platelet activation status as well as proinflammatory condition in type 1 diabetes. Here, in the present study, we observed an increase in macrophage and platelet interaction at late stages of diabetes compared to control, whereas, after AMS treatment, diabetic rats showed fewer macrophage and platelet interactions compared to diabetes. The study suggests that AMS can reduce the macrophage and platelet interaction and can further inhibit pro-inflammatory conditions which leads to vascular complications in diabetes.

Additionally, it has been suggested that abnormal platelet metabolism and alterations to intraplatelet signaling pathways may be involved in the pathophysiology of atherothrombotic events in diabetes (95). To explore the mechanism behind the altered platelet parameters and similarly the pathway behind the beneficial effect of AMS, we performed a metabolomics study. We found arachidonic acid pathway with highly altered metabolites in diabetes. In support of our results, a study has shown that the altered arachidonic acid metabolism is presenting platelets in diabetes patients with coronary artery disease (103). We found arachidonic acid metabolites namely 13,14-dihydro-15-keto Prostaglandin F2alpha, 7-hydroxy docosahexaenoic acid, Prostaglandin E2 and 15-HETE downregulated in diabetes which has been further effectively upregulated by AMS. This suggests the beneficial role of AMS is through modulating arachidonic acid pathway.

Apart from diabetes, the recent well-known cardiometabolic disease is NAFLD (26). The pathophysiology of NAFLD involves several pathways which interlinked in a complex way and therefore, make the disease difficult to understand (27). PTMs of proteins such as acetylation play a crucial role in regulating various protein functions and maintaining cellular homeostasis (104). In the liver, protein acetylation regulates several metabolic pathways such as glucose and lipid metabolism (105,106). Previous studies showed that the alteration in the acetylation of proteins may lead to fatty liver disease (107,108). Further, recent findings highlighted the significance of lysine acetylation on subcellular distribution, transcriptional activity, DNA affinity, and stability of transcription factors (109). Therefore, understanding the acetylation of transcription factors in NAFLD may add strength to existing pathophysiology.

Numerous investigations have shown that vitamin D insufficiency is associated with both a higher frequency of NAFLD and a higher grade of NAFLD severity (110). The expression of VDR in hepatic cells generally helps to reduce inflammation in chronic hepatitis (35). Paricalcitol, a vitamin D analog and drug to treat hyperparathyroidism in patients with chronic kidney disease (111), could be a promising therapeutic agent to treat NAFLD. Study prevented the accumulation of fat in liver cells (112). Further, paricalcitol prevented fibrosis in carbon tetrachloride (CCL4) induced chronic liver disease model in rats (113). Previously, paricalcitol showed its beneficial effect by reducing oxidative stress and inflammation in

diabetes, kidney diseases, and cardiovascular diseases (114–116). However, the role of paricalcitol in regulating inflammation and oxidative stress in NAFLD is still not evaluated. Therefore, the present study tried to explore the effect of paricalcitol in attenuating oxidative stress and inflammation in an *in-vivo* rat model of NAFLD, and the molecular mechanism thereof.

We developed a NAFLD rat model by administration of a choline-deficient high-fat (CDHF) diet (117). To find the efficacy, paricalcitol was administered to NAFLD rats after 12 weeks of the CDHF diet at a dose of 0.08μg/kg/day by intraperitoneal route for a period of 8 weeks. Although there was an increase in body weight and a decrease in food intake in NAFLD rats compared to the control, there were no changes in both parameters after paricalcitol treatment to NAFLD rats. Further, we measured the serum level of liver injury markers such as AST and ALT. Previous studies showed that elevated ALT and AST are known as surrogate markers of the disease, NAFLD (118). Another study showed that calcitriol, a vitamin D analog reduced the ALT and AST in NAFLD patients (119). Moreover, in the present study, the elevated ALT and AST in NAFLD have been effectively reduced by paricalcitol suggesting paricalcitol's role in decreasing liver injury in NAFLD. Apart from transaminases, uric acid is also known to be associated with the occurrence and progression of NAFLD. According to a study, elevated uric acid was found in patients with NAFLD and can be used as a predictor of disease (120). Similarly, recent research showed a beneficial effect of paricalcitol in reducing uric acid levels in diabetic nephropathy (121). Although increased uric acid levels were found in NAFLD rats, paricalcitol did not show any effect on uric acid levels. NAFLD is also known to be associated with insulin resistance and hyperinsulinemia which stimulates lipogenesis by SREBP-1c in NAFLD liver (122,123)**.** Paricalcitol effectively reduced the insulin in serum suggesting a beneficial role of paricalcitol in NAFLD**.** Further, a previous study showed that paricalcitol enhances insulin sensitivity in Type 2 diabetes (124)**.** A large proportion of NAFLD patients are known to be accompanied by dyslipidemia (125)**.** Increased serum lipids such as TG, LDL, cholesterol, and decreased HDL were linked with increasing degrees of fatty liver (126)**.** As expected, vitamin D deficiency is also linked with dyslipidemia in NAFLD (110). In the present study, we observed elevated TG, LDL, and decreased HDL in NAFLD rats which were reduced by paricalcitol treatment suggesting paricalcitol attenuates dyslipidemia in NAFLD.

According to a study, exposure to a high-fat diet (HFD) increased the acetylation of proteins involved in gluconeogenesis, methionine metabolism, mitochondrial oxidative metabolism, endoplasmic reticulum (ER) stress response, and liver damage (127). In the present study, acetylation status in NAFLD liver was observed by western blot. Increased lysine acetylation of hepatic proteins in NAFLD rats was effectively reversed by paricalcitol treatment. It is well-known that the increased acetylation is associated with a decrease in sirtuins activity or protein levels. Among all sirtuins, SIRT1 and SIRT3 are the major players in regulating protein acetylation in the nucleus, cytoplasm, and mitochondria (128). Also, studies showed a

strong relationship between sirtuins and the development of NAFLD (129,130). Further, we measured the expression of SIRT1 and SIRT3 which are the major SIRTs involved in the acetylation of proteins involved in cell metabolism (131).

In the present study, we observed that SIRT1 and SIRT3 protein expression is significantly downregulated in NAFLD disease condition when compared to the control group, suggesting the increased acetylation is due to a decreased deacetylase activity in the liver of NAFLD rats. Further, NAFLD treated with the paricalcitol showed an upregulation in both SIRT1 and SIRT3 expression indicating an increase in deacetylation activity. A study proved that the downregulation of SIRT1 and SIRT3 caused by excessive fat intake increases lipotoxicity, ROS production, mitochondrial damage, apoptosis, and inflammatory responses in the liver leading to cell injury (132,133). Further, a study showed that paricalcitol reduces cholestatic liver damage by activating the SIRT1 pathway (36). Vitamin D supplementation has effectively increased the level of SIRT1 in the serum of diabetic patients (134). Further vitamin D supplement has also elevated SIRT3 in HFD-fed rats (135). All the above studies suggest that paricalcitol has the property to attenuate elevated acetylation of proteins in NAFLD by activating the SIRT1 and SIRT3 pathways.
Moreover, sirtuins are well known to affect the function of several transcription factors and regulate cell function (136). One of the important downstream targets of SIRT1 is NFκB which regulates inflammation in cells (137). Expression of total and acetylated NFκB was upregulated in the liver of NAFLD rats and downregulated in the paricalcitol-treated group. This data indicates that the hepatic inflammation increased in the NAFLD rats and decreased after paricalcitol treatment. As site-specific acetylation of NFκB (K310) increases its binding to the DNA promoter regions and enhanced expression of several proinflammatory cytokines (138,139), we measured mRNA expression of several inflammatory genes like TNFα, IL-1ß, and NFκB. TNFα is a pleiotropic cytokine that regulates pathways involved in the regulation of inflammation, cell metabolism, and tissue homeostasis (140). IL-1ß is a pro-inflammatory cytokine that can disrupt lipid signaling pathways in lipid metabolism (141). Besides that, these genes are responsible for causing liver fibrosis, steatosis, and inflammation (142,143). As a primary regulator in the inflammatory response, NFκB can be targeted to reduce inflammation in NAFLD. (144). The present study showed that all three inflammatory genes were significantly upregulated in the liver of NAFLD rats when compared to the control. However, paricalcitol treatment significantly downregulated the expression of all three inflammatory markers. Similar to our study, a previous study showed that paricalcitol treatment reduced hepatic ischemia/reperfusion injury in rats by down-regulating the TLR4 signaling pathway (145). Further, it is well known that TLR 4 activation is involved in NFκB mediated inflammatory responses in the liver (146). Therefore, the decreased inflammatory response of paricalcitol showed in the present study is due to decreased acetylation activation of NFκB, thereby inhibiting the expression of inflammatory genes. Additionally, a recent study showed that the inflammatory process in NAFLD is also mediated by an

elevated myeloperoxidase (MPO) by Kuffer cells which leads to an increased CXC chemokine and neutrophile infiltration, and causes MPO-mediated liver damage (147). In the present study, we observed an elevated MPO in the liver was effectively reduced by paricalcitol. Further, increased hepatic ballooning and inflammation in the liver of NAFLD rats were also attenuated by paricalcitol. Together the study proved the anti-inflammatory properties of paricalcitol in NAFLD.

The present study also evaluated FOXO3A, one important transcription factor that activates several antioxidant genes and is modulated by both SIRT1 and SIRT3 for its regulation (148,149). Studies showed that FOXO3A is deacetylated by SIRT3 to prevent it from being phosphorylated, ubiquitinated, or degraded, which stabilizes FOXO3A proteins (150). Studies also showed a decreased FOXO3A expression is associated with fatty liver disease and hepatitis C (147,151). In the present study, the expression of acetylated FOXO3A and total FOXO3A is upregulated in the liver of NAFLD rats. Although previous studies showed decreased FOXO3A in NAFLD, here in the present study, we suggest that the increased total FOXO3A observed may be due to an increased acetylated FOXO3A. Further, treatment with paricalcitol attenuated the FOXO3A acetylation in the NAFLD liver suggesting an important role of paricalcitol in attenuating FOXO3A acetylation. In defense of oxidative stress, FOXO3A transcriptionally binds to promotors of antioxidant genes such as mitochondrial manganese superoxide dismutase (MnSOD) and catalase and increases their expression (152). Moreover, MnSOD, catalase, and GSH neutralize superoxide radicals and hydrogen peroxide and play an important role in protecting cells from oxidative stress (153). Further, we checked the mRNA expression of the catalase and MnSOD which was found to be decreased in NAFLD and increased after paricalcitol treatment. Similarly, the hepatic antioxidant activity of catalase and GSH concentration were decreased in NAFLD rats but significantly improved after paricalcitol treatment. This suggests that the acetylation of FOXO3A attenuated the transcriptional activation of antioxidant genes which may further promote oxidative stress. Paricalcitol effectively reversed the oxidative stress condition in NAFLD. Further to prove this, we calculated the total antioxidant level in the rat liver. The percentage of total antioxidant activity in the liver was significantly reduced in the NAFLD rats but increased after paricalcitol treatment. Further, it was known that an increased ROS may lead to liver damage in NAFLD (154). In the present study, hepatic ROS measured by DCFDA was increased in NAFLD rats but reduced significantly after paricalcitol treatment. This suggests that paricalcitol effectively inhibited the oxidative stress in NAFLD. Increased antioxidant activity in NAFLD liver paricalcitol not only reduces oxidative stress, it also maintains an optimum level of the ROS in the liver which is essential for cellular signaling processes. Further, ROS would trigger lipid peroxidation followed by activation of the inflammatory response (155). Previously it was proved that increased lipid peroxidation, an indicator of oxidative stress is associated with NAFLD progression (156). This study showed that lipid peroxidation of liver was increased in NAFLD rats, and reduced after paricalcitol treatment.

Further, we tried to see the effect of paricalcitol on cardiac function. Previous studies showed an association of subclinical changes in cardiac structure and function with NAFLD over time (157). In this study, we for the first time demonstrated that treatment with paricalcitol is protective against the cardiac hypertrophic stimulus due to a choline-deficient high-fat diet. Indeed, paricalcitol ameliorated the CDHF-induced cardiac enlargements determined by examination of heart weight to body weight ratio, and echocardiography. In our study, we observed an increase in the cardiac wall thickness and decreased lumen size of the left ventricle in diastole. Further, we observed an increase in heart weight as well as LV mass in NAFLD rats. This suggests a condition of left ventricular hypertrophy where an increased ventricular wall thickness is initially observed followed by an increased LV mass (158). This is due to accumulation of the lipids in the cells of the left ventricle myocardium which may cause concentric hypertrophy (159). Further, we observed a decrease in ejection fraction in NAFLD. Studies showed an association of NAFLD with a higher risk of heart failure with reduced ejection fraction and heart failure with preserved ejection fraction (160). In our study, paricalcitol treatment has effectively reversed these conditions in the heart at the 16^{th} as well as 20^{th} week of CDHF-induced NAFLD. This suggests that paricalcitol could be used as a food supplement for preventing pathological heart disease.

In summary, we showed the effectiveness of AMS as well as paricalcitol in cardiometabolic diseases such as diabetes and NAFLD respectively. In diabetes, AMS, a naturally derived metabolite of garlic can be considered a safe and effective therapeutic strategy when compared to chemical drugs such as aspirin in attenuating diabetes and its CVD. AMS shows its effect by inhibiting the activation, and aggregation of platelets. Further AMS can attenuate the inflammation process in the vascular system by inhibiting the macrophage-platelet interaction as well as endogenous ROS production. Metabolomics data further revealed that AMS may inhibit platelet activation by modulating arachidonic acid pathway. Similarly, we have explored paricalcitol, an FDA-approved drug for renal failure, in an NAFLD model and established its efficacy by looking at its ability to reverse protein acetylation, especially NFκB, and FOXO3A. Further, paricalcitol effectively reduced cardiac dysfunction. The present study has shown the potential to repurpose the drug paricalcitol, well-known for its use in renal failure, in NAFLD as well as in its associated cardiac complications.

6. Impact of research in the advancement of knowledge and benefit to mankind

As diabetes is very common among world populations, there is a need for safe and effective treatment strategies. Stroke and heart attack are two most serious events influenced by diabetes. To reduce the burden of stroke and heart attack, recent research focused on the activation of platelets in diabetes which ultimately led to the development of cardiovascular events. This makes the need for potential antiplatelet drugs in diabetes. Natural compound which is safe and affordable and has great potential as drugs has been explored in preventing diabetes and its complications. Unlike the known antiplatelet drugs such as aspirin, allyl methyl sulfide could be the safe and effective drug of choice with no adverse reactions in treating diabetes patients. Allyl methyl sulfide is derived from the natural source of garlic and present in blood when we consumed; hence it can be translated easily to humans. Further, the dual role of AMS on both glycemic control and antiplatelet properties makes this molecule a preventive treatment for diabetic as well as diabetes-related cardiovascular complications. Moreover, research on optimizing the dose of AMS for clinical use may be further helpful.

NAFLD is a recent global burden among chronic liver disease which is known to be associated with cardiometabolic dysfunction. Because of the disease's complexity, there is a lack of clear views on NAFLD pathogenesis. In our study, we showed the role of post-translational modification (acetylation) of proteins in NAFLD pathogenesis by increasing the acetylation of NFkB and FOXO3A. Our research on the role of protein acetylation in NAFLD has strengthened the existing pathophysiology of NAFLD**.** Further paricalcitol, a vitamin D analog has effectively reversed the acetylation of protein in NAFLD. This helps to understand the importance of acetylation of proteins in NAFLD disease development as well as the beneficial role of paricalcitol in reversing the increased acetylation in the liver. Further, our research has shown a cardio-protective action of paricalcitol in NAFLD. This together makes paricalcitol a potential drug to treat the liver-heart axis in NAFLD. As paricalcitol has already been approved for chronic kidney disease, repurposing of paricalcitol in NAFLD can be translated to humans easily.

Therefore, my study has a great potential to translate in human without any regulatory hurdles. I am looking forward to translating the preclinical data in clinical settings.

7. References:

1. Guo F, Moellering DR, Garvey WT. The progression of cardiometabolic disease: validation of a new cardiometabolic disease staging system applicable to obesity. Obes Silver Spring Md. 2014 Jan;22(1):110–8.

2. de Waard AKM, Hollander M, Korevaar JC, Nielen MMJ, Carlsson AC, Lionis C, et al. Selective prevention of cardiometabolic diseases: activities and attitudes of general practitioners across Europe. Eur J Public Health. 2019 Feb 1;29(1):88–93.

3. Ndisang JF, Rastogi S. Cardiometabolic Diseases and Related Complications: Current Status and Future Perspective. BioMed Res Int. 2013;2013:467682.

4. Choi MR. Inside the pathophysiological mechanisms of cardiometabolic diseases: the other pandemic to fight. Pflüg Arch - Eur J Physiol. 2022 Jan 1;474(1):1–4.

5. De Rosa S, Arcidiacono B, Chiefari E, Brunetti A, Indolfi C, Foti DP. Type 2 Diabetes Mellitus and Cardiovascular Disease: Genetic and Epigenetic Links. Front Endocrinol [Internet]. 2018 [cited 2023 Aug 26];9. Available from: https://www.frontiersin.org/articles/10.3389/fendo.2018.00002

6. Kubisz P, Stančiaková L, Staško J, Galajda P, Mokáň M. Endothelial and platelet markers in diabetes mellitus type 2. World J Diabetes. 2015 Apr 15;6(3):423–31.

7. Beckman JA, Creager MA, Libby P. Diabetes and atherosclerosis: epidemiology, pathophysiology, and management. JAMA. 2002 May 15;287(19):2570–81.

8. Fidler TP, Marti A, Gerth K, Middleton EA, Campbell RA, Rondina MT, et al. Glucose Metabolism Is Required for Platelet Hyperactivation in a Murine Model of Type 1 Diabetes. Diabetes. 2019 May;68(5):932–8.

9. Wang B, Yee Aw T, Stokes KY. N-acetylcysteine attenuates systemic platelet activation and cerebral vessel thrombosis in diabetes. Redox Biol. 2017 Sep 20;14:218–28.

10. Bhatt DL. Antiplatelet therapy following myocardial infarction in patients with diabetes. JAMA. 2012 Sep 5;308(9):921–2.

11. Capodanno D, Angiolillo DJ. Antithrombotic Therapy for Atherosclerotic Cardiovascular Disease Risk Mitigation in Patients With Coronary Artery Disease and Diabetes Mellitus. Circulation. 2020 Dec;142(22):2172–88.

12. Boccardi A, Shubrook JH. Cutaneous Reactions to Antidiabetic Agents: A Narrative Review. Diabetology. 2022 Mar;3(1):97–107.

13. Day C. Traditional plant treatments for diabetes mellitus: pharmaceutical foods. Br J Nutr. 1998 Jul;80(1):5–6.

14. S. Patumraj, S. Tewit, S. Amatyakul. Comparative Effects of Garlic and Aspirin on Diabetic Cardiovascular Complications. Drug Deliv. 2000 Jan;7(2):91–6.

15. Eidi A, Eidi M, Esmaeili E. Antidiabetic effect of garlic (Allium sativum L.) in normal and streptozotocin-induced diabetic rats. Phytomedicine. 2006 Nov 24;13(9):624–9.

16. Padiya R, Khatua TN, Bagul PK, Kuncha M, Banerjee SK. Garlic improves insulin sensitivity and associated metabolic syndromes in fructose fed rats. Nutr Metab. 2011 Jul 27;8(1):53.

17. Cavagnaro PF, Camargo A, Galmarini CR, Simon PW. Effect of cooking on garlic (Allium sativum L.) antiplatelet activity and thiosulfinates content. J Agric Food Chem. 2007 Feb 21;55(4):1280–8.

18. Fukao H, Yoshida H, Tazawa Y ichi, Hada T. Antithrombotic Effects of Odorless Garlic Powder Both *in Vitro* and *in Vivo*. Biosci Biotechnol Biochem. 2007 Jan 23;71(1):84–90.

19. Hattori A, Yamada N, Nishikawa T, Fukuda H, Fujino T. Antidiabetic effects of ajoene in genetically diabetic KK-A(y) mice. J Nutr Sci Vitaminol (Tokyo). 2005 Oct;51(5):382–4.

20. Sheela CG, Augusti KT. Antidiabetic effects of S-allyl cysteine sulphoxide isolated from garlic Allium sativum Linn. Indian J Exp Biol. 1992 Jun;30(6):523–6.

21. Sujithra K, Srinivasan S, Indumathi D, Vinothkumar V. Allyl methyl sulfide, an organosulfur compound alleviates hyperglycemia mediated hepatic oxidative stress and inflammation in streptozotocin - induced experimental rats. Biomed Pharmacother Biomedecine Pharmacother. 2018 Nov;107:292–302.

22. Rosen RobertT, Hiserodt RD, Fukuda EK, Ruiz RJ, Zhou Z, Lech J, et al. Determination of Allicin, S-Allylcysteine and Volatile Metabolites of Garlic in Breath, Plasma or Simulated Gastric Fluids. J Nutr. 2001 Mar 1;131(3):968S-971S.

23. Mohammed SA, Paramesha B, Kumar Y, Tariq U, Arava SK, Banerjee SK. Allylmethylsulfide, a Sulfur Compound Derived from Garlic, Attenuates Isoproterenol-Induced Cardiac Hypertrophy in Rats. Oxid Med Cell Longev. 2020 Jun 12;2020:1–15.

24. Khatua TN, Borkar RM, Mohammed SA, Dinda AK, Srinivas R, Banerjee SK. Novel Sulfur Metabolites of Garlic Attenuate Cardiac Hypertrophy and Remodeling through Induction of Na+/K+-ATPase Expression. Front Pharmacol. 2017 Jan 30;8:18.

25. Lim S, Taskinen MR, Borén J. Crosstalk between nonalcoholic fatty liver disease and cardiometabolic syndrome. Obes Rev. 2019;20(4):599–611.

26. Lakhani HV, Sharma D, Dodrill MW, Nawab A, Sharma N, Cottrill CL, et al. Phenotypic Alteration of Hepatocytes in Non-Alcoholic Fatty Liver Disease. Int J Med Sci. 2018 Oct 20;15(14):1591–9.

27. Marchisello S, Di Pino A, Scicali R, Urbano F, Piro S, Purrello F, et al. Pathophysiological, Molecular and Therapeutic Issues of Nonalcoholic Fatty Liver Disease: An Overview. Int J Mol Sci. 2019 Apr 20;20(8):1948.

28. Muzurović E, Peng CCH, Belanger MJ, Sanoudou D, Mikhailidis DP, Mantzoros CS. Nonalcoholic Fatty Liver Disease and Cardiovascular Disease: a Review of Shared Cardiometabolic Risk Factors. Hypertension. 2022 Jul;79(7):1319–26.

29. Targher G, Byrne CD, Lonardo A, Zoppini G, Barbui C. Non-alcoholic fatty liver disease and risk of incident cardiovascular disease: A meta-analysis. J Hepatol. 2016 Sep;65(3):589–600.

30. Smeuninx B, Boslem E, Febbraio MA. Current and Future Treatments in the Fight against Non-Alcoholic Fatty Liver Disease. Cancers. 2020 Jun 28;12(7):1714.

31. Parker J, Hashmi O, Dutton D, Mavrodaris A, Stranges S, Kandala NB, et al. Levels of vitamin D and cardiometabolic disorders: Systematic review and meta-analysis. Maturitas. 2010 Mar 1;65(3):225–36.

32. Wang Q, Shi X, Wang J, Zhang J, Xu C. Low serum vitamin D concentrations are associated with obese but not lean NAFLD: a cross-sectional study. Nutr J. 2021 Apr 1;20(1):30.

33. Zhang H, Shen Z, Lin Y, Zhang J, Zhang Y, Liu P, et al. Vitamin D receptor targets hepatocyte nuclear factor 4α and mediates protective effects of vitamin D in nonalcoholic fatty liver disease. J Biol Chem. 2020 Mar 20;295(12):3891–905.

34. Zhang R, Wang M, Wang M, Zhang L, Ding Y, Tang Z, et al. Vitamin D Level and Vitamin D Receptor Genetic Variation Were Involved in the Risk of Non-Alcoholic Fatty Liver Disease: A Case-Control Study. Front Endocrinol. 2021 Aug 6;12:648844.

35. Barchetta I, Carotti S, Labbadia G, Gentilucci UV, Muda AO, Angelico F, et al. Liver vitamin D receptor, CYP2R1, and CYP27A1 expression: relationship with liver histology and vitamin D3 levels in patients with nonalcoholic steatohepatitis or hepatitis C virus. Hepatol Baltim Md. 2012 Dec;56(6):2180–7.

36. Jia R, Yang F, Yan P, Ma L, Yang L, Li L. Paricalcitol inhibits oxidative stress-induced cell senescence of the bile duct epithelium dependent on modulating Sirt1 pathway in cholestatic mice. Free Radic Biol Med. 2021 Jun 1;169:158–68.

37. Alborzi P, Patel NA, Peterson C, Bills JE, Bekele DM, Bunaye Z, et al. Paricalcitol Reduces Albuminuria and Inflammation in Chronic Kidney Disease. Hypertension. 2008 Aug;52(2):249–55.

38. Demir M, İçaçan G, Yakar B, Doğukan A. The effect of paricalcitol on Hepatitis B immunization in hemodialysis patients: The effect of paricalcitol on Hepatitis B immunization. Med Sci Discov. 2020 Jul 16;7(7):549–53.

39. Mohammed SA, Paramesha B, Meghwani H, Kumar Reddy MP, Arava SK, Banerjee SK. Allyl Methyl Sulfide Preserved Pressure Overload-Induced Heart Failure Via Modulation of Mitochondrial Function. Biomed Pharmacother. 2021 Jun 1;138:111316.

40. De Cuyper IM, Meinders M, van de Vijver E, de Korte D, Porcelijn L, de Haas M, et al. A novel flow cytometry–based platelet aggregation assay. Blood. 2013 Mar 7;121(10):e70–80.

41. Genin M, Clement F, Fattaccioli A, Raes M, Michiels C. M1 and M2 macrophages derived from THP-1 cells differentially modulate the response of cancer cells to etoposide. BMC Cancer. 2015 Aug 8;15(1):577.

42. Mehrpouri M, Bashash D, Mohammadi MH, Gheydari ME, Satlsar ES, Hamidpour M. Co-culture of Platelets with Monocytes Induced M2 Macrophage Polarization and Formation of Foam Cells:

Shedding Light on the Crucial Role of Platelets in Monocyte Differentiation. Turk J Hematol. 2019 Jun;36(2):97–105.

43. Walsh TG, Berndt MC, Carrim N, Cowman J, Kenny D, Metharom P. The role of Nox1 and Nox2 in GPVI-dependent platelet activation and thrombus formation. Redox Biol. 2014;2:178–86.

44. Carrim N, Arthur JF, Hamilton JR, Gardiner EE, Andrews RK, Moran N, et al. Thrombin-induced reactive oxygen species generation in platelets: A novel role for protease-activated receptor 4 and GPIbα. Redox Biol. 2015 Dec;6:640–7.

45. Bagul PK, Dinda AK, Banerjee SK. Effect of resveratrol on sirtuins expression and cardiac complications in diabetes. Biochem Biophys Res Commun. 2015 Dec;468(1–2):221–7.

46. Katare P, Lateef Nizami H, Paramesh B, Dinda A, Banerjee S. Activation of toll like receptor 4 (TLR4) promotes cardiomyocyte apoptosis through SIRT2 dependent p53 deacetylation. Sci Rep. 2020 Nov 6;10.

47. Ohkawa H, Ohishi N, Yagi K. Assay for lipid peroxides in animal tissues by thiobarbituric acid reaction. Anal Biochem. 1979 Jun 1;95(2):351–8.

48. Ellman GL. Tissue sulfhydryl groups. Arch Biochem Biophys. 1959 May;82(1):70–7.

49. Aebi H. Catalase. In: Bergmeyer HU, editor. Methods of Enzymatic Analysis (Second Edition) [Internet]. Academic Press; 1974 [cited 2023 Aug 9]. p. 673–84. Available from: https://www.sciencedirect.com/science/article/pii/B9780120913022500323

50. Zahin M, Aqil F, Ahmad I. The in vitro antioxidant activity and total phenolic content of four Indian medicinal plants. Int J Pharm Pharm Sci. 2009;1(SUPPL. 1):88–95.

51. Maity P, Bindu S, Dey S, Goyal M, Alam A, Pal C, et al. Indomethacin, a Non-steroidal Anti-inflammatory Drug, Develops Gastropathy by Inducing Reactive Oxygen Species-mediated Mitochondrial Pathology and Associated Apoptosis in Gastric Mucosa: A NOVEL ROLE OF MITOCHONDRIAL ACONITASE OXIDATION*. J Biol Chem. 2009 Jan 30;284(5):3058–68.

52. Krawisz JE, Sharon P, Stenson WF. Quantitative assay for acute intestinal inflammation based on myeloperoxidase activity. Gastroenterology. 1984 Dec;87(6):1344–50.

53. Cho NH, Becker DJ, Ellis D, Kuller LH, Drash AL, Orchard TJ. Spontaneous whole blood platelet aggregation, hematological variables and complications in insulin-dependent diabetes mellitus: The Pittsburgh Epidemiology of Diabetes Complications Study. J Diabetes Complications. 1992 Jan 1;6(1):12–8.

54. Agardh CD, Agardh E, Bauer B. Platelet aggregation in Type I diabetics with and without proliferative retinopathy. Acta Ophthalmol (Copenh). 2009 May 27;65(3):358–62.

55. Dharmalingam M, Yamasandhi PG. Nonalcoholic Fatty Liver Disease and Type 2 Diabetes Mellitus. Indian J Endocrinol Metab. 2018;22(3):421–8.

56. Khandelwal R, Dassanayake AS, Conjeevaram HS, Singh SP. Non-alcoholic fatty liver disease in diabetes: When to refer to the hepatologist? World J Diabetes. 2021 Sep 15;12(9):1479–93.

57. Caussy C, Aubin A, Loomba R. The Relationship Between Type 2 Diabetes, NAFLD, and Cardiovascular Risk. Curr Diab Rep. 2021 Mar 19;21(5):15.

58. Chillarón JJ, Flores Le-Roux JA, Benaiges D, Pedro-Botet J. Type 1 diabetes, metabolic syndrome and cardiovascular risk. Metabolism. 2014 Feb;63(2):181–7.

59. Fredman G, Ozcan L, Tabas I. Common Therapeutic Targets in Cardiometabolic Disease. Sci Transl Med. 2014 Jun 4;6(239):239ps5.

60. Bebu I, Braffett BH, Pop-Busui R, Orchard TJ, Nathan DM, Lachin JM, et al. The relationship of blood glucose with cardiovascular disease is mediated over time by traditional risk factors in type 1 diabetes: the DCCT/EDIC study. Diabetologia. 2017 Oct 1;60(10):2084–91.

61. Lind M, Svensson AM, Kosiborod M, Gudbjörnsdottir S, Pivodic A, Wedel H, et al. Glycemic Control and Excess Mortality in Type 1 Diabetes. N Engl J Med. 2014 Nov 20;371(21):1972–82.

62. Sousa GR, Pober D, Galderisi A, Lv H, Yu L, Pereira AC, et al. Glycemic Control, Cardiac Autoimmunity, and Long-Term Risk of Cardiovascular Disease in Type 1 Diabetes: A DCCT/EDIC Cohort-Based Study. Circulation. 2019 Feb 5;139(6):730–43.

63. Mona HM, Sahar SA, Hend SM, Nanees AWA. Dyslipidemia in type 1 diabetes mellitus: Relation to diabetes duration, glycemic control, body habitus, dietary intake and other epidemiological risk factors. Egypt Pediatr Assoc Gaz. 2015 Jun 1;63(2):63–8.

64. Rahma S, Rashid JA, Farage AHA. The Significance of Lipid Abnormalities in Children with Insulin-Dependant Diabetes Mellitus. 2006;6.

65. Lechleitner M, Koch T, Herold M, Dzien A, Hoppichler F. Tumour necrosis factor-alpha plasma level in patients with type 1 diabetes mellitus and its association with glycaemic control and cardiovascular risk factors. J Intern Med. 2000;248(1):67–76.

66. Tsalamandris S, Antonopoulos AS, Oikonomou E, Papamikroulis GA, Vogiatzi G, Papaioannou S, et al. The Role of Inflammation in Diabetes: Current Concepts and Future Perspectives. Eur Cardiol Rev. 2019 Apr;14(1):50–9.

67. Martín-Gallán P, Carrascosa A, Gussinyé M, Domínguez C. Biomarkers of diabetes-associated oxidative stress and antioxidant status in young diabetic patients with or without subclinical complications. Free Radic Biol Med. 2003 Jun 15;34(12):1563–74.

68. Marra G, Cotroneo P, Pitocco D, Manto A, Leo MASD, Ruotolo V, et al. Early Increase of Oxidative Stress and Reduced Antioxidant Defenses in Patients With Uncomplicated Type 1 Diabetes: A case for gender difference. Diabetes Care. 2002 Feb 1;25(2):370–5.

69. Alessandrini P, McRae J, Feman S, FitzGerald GA. Thromboxane Biosynthesis and Platelet Function in Type I Diabetes Mellitus. N Engl J Med. 1988 Jul 28;319(4):208–12.

70. Pd W, C W, Rl KR. Membrane fluidity is related to the extent of glycation of proteins, but not to alterations in the cholesterol to phospholipid molar ratio in isolated platelet membranes from diabetic and control subjects. Thromb Haemost. 1992 May 1;67(5):567–71.

71. Calverley DC, Hacker MR, Loda KA, Brass E, Buchanan TA, Tsao-Wei DD, et al. Increased platelet Fc receptor expression as a potential contributing cause of platelet hypersensitivity to collagen in diabetes mellitus. Br J Haematol. 2003;121(1):139–42.

72. Santilli F, Simeone P, Liani R. 27 - The Role of Platelets in Diabetes Mellitus. In: Michelson AD, editor. Platelets (Fourth Edition) [Internet]. Academic Press; 2019 [cited 2021 Aug 2]. p. 469–503. Available from: https://www.sciencedirect.com/science/article/pii/B9780128134566000278

73. Lee P, Jenkins A, Bourke C, Santamaria J, Paton C, Janus E, et al. Prothrombotic and Antithrombotic Factors are Elevated in Patients with Type 1 Diabetes Complicated by Microalbuminuria. Diabet Med. 1993 Mar;10(2):122–8.

74. Padiya R, Banerjee S. Garlic as an Anti-diabetic Agent: Recent Progress and Patent Reviews. Recent Pat Food Nutr Agric. 2012 Dec 24;5.

75. Patumraj S, Tewit S, Amatyakul S, Jariyapongskul A, Maneesri S, Kasantikul V, et al. Comparative effects of garlic and aspirin on diabetic cardiovascular complications. Drug Deliv. 2000 Jun;7(2):91–6.

76. Cavagnaro P, Camargo A, Galmarini C, Simon P. Effect of Cooking on Garlic (Allium sativum L.) Antiplatelet Activity and Thiosulfinates Content. J Agric Food Chem. 2007 Mar 1;55:1280–8.

77. Block E, Bechand B, Gundala S, Vattekkatte A, Wang K, Mousa SS, et al. Fluorinated Analogs of Organosulfur Compounds from Garlic (Allium sativum): Synthesis, Chemistry and Anti-Angiogenesis and Antithrombotic Studies. Molecules. 2017 Dec;22(12):2081.

78. Ariga T, Seki T. Antithrombotic and anticancer effects of garlic-derived sulfur compounds: a review. BioFactors Oxf Engl. 2006;26(2):93–103.

79. Rosen RobertT, Hiserodt RD, Fukuda EK, Ruiz RJ, Zhou Z, Lech J, et al. Determination of Allicin, S-Allylcysteine and Volatile Metabolites of Garlic in Breath, Plasma or Simulated Gastric Fluids. J Nutr. 2001 Apr 1;131(3):968S-971S.

80. Sujithra K, Srinivasan S, Indumathi D, Vinothkumar V. Allyl methyl sulfide, an organosulfur compound alleviates hyperglycemia mediated hepatic oxidative stress and inflammation in streptozotocin - induced experimental rats. Biomed Pharmacother. 2018 Nov 1;107:292–302.

81. Sujithra K, Srinivasan S, Indumathi D, Vinothkumar V. Allyl methyl sulfide, a garlic active component mitigates hyperglycemia by restoration of circulatory antioxidant status and attenuating glycoprotein components in streptozotocin-induced experimental rats. Toxicol Mech Methods. 2019 Mar 24;29(3):165–76.

82. Coe LM, Denison JD, McCabe LR. Low dose aspirin therapy decreases blood glucose levels but does not prevent type i diabetes-induced bone loss. Cell Physiol Biochem Int J Exp Cell Physiol Biochem Pharmacol. 2011;28(5):923–32.

83. Banerjee SK, Maulik M, Manchanda SC, Dinda AK, Das TK, Maulik SK. Garlic-induced alteration in rat liver and kidney morphology and associated changes in endogenous antioxidant status. Food Chem Toxicol. 2001 Aug;39(8):793–7.

84. Schneider DJ. Factors Contributing to Increased Platelet Reactivity in People With Diabetes. Diabetes Care. 2009 Apr 1;32(4):525–7.

85. Venkatesh V, Kumar R, Varma DK, Bhatia P, Yadav J, Dayal D. Changes in platelet morphology indices in relation to duration of disease and glycemic control in children with type 1 diabetes mellitus. J Diabetes Complications. 2018 Sep 1;32(9):833–8.

86. Zahran AM, El-Badawy O, Mohamad IL, Tamer DM, Abdel-Aziz SM, Elsayh KI. Platelet Activation and Platelet–Leukocyte Aggregates in Type I Diabetes Mellitus. Clin Appl Thromb. 2018 Dec;24(9 Suppl):230S-239S.

87. Tarnow I, Michelson AD, Barnard MR, Frelinger AL, Aasted B, Jensen BR, et al. Nephropathy in Type 1 diabetes is associated with increased circulating activated platelets and platelet hyperreactivity. Platelets. 2009 Jan 1;20(7):513–9.

88. Halushka PV, Rogers RC, Loadholt CB, Colwell JA. Increased platelet thromboxane synthesis in diabetes mellitus. J Lab Clin Med. 1981 Jan;97(1):87–96.

89. Heath H, Bbigden WD, Canever JV, Pollock J, Hunter PR, Kelsey J, et al. Platelet adhesiveness and aggregation in relation to diabetic retinopathy. Diabetologia. 1971 Oct;7(5):308–15.

90. Schäfer A, Bauersachs J. Endothelial dysfunction, impaired endogenous platelet inhibition and platelet activation in diabetes and atherosclerosis. Curr Vasc Pharmacol. 2008 Jan;6(1):52–60.

91. Anfossi G, Mularoni EM, Burzacca S, Ponziani MC, Massucco P, Mattiello L, et al. Platelet resistance to nitrates in obesity and obese NIDDM, and normal platelet sensitivity to both insulin and nitrates in lean NIDDM. Diabetes Care. 1998 Jan;21(1):121–6.

92. Chirkov II, Tyshchiuk IA, Severina IS, Starosel'tseva LK. [ADP-induced aggregation of human platelets in diabetes mellitus]. Vopr Med Khim. 1990 Aug;36(4):20–2.

93. Mahmoodian R, Salimian M, Hamidpour M, Khadem-Maboudi AA, Gharehbaghian A. The effect of mild agonist stimulation on the platelet reactivity in patients with type 2 diabetes mellitus. BMC Endocr Disord. 2019 Jun 14;19(1):62.

94. Kasjanovová D, Baláz V. Age-related changes in human platelet function in vitro. Mech Ageing Dev. 1986 Dec;37(2):175–82.

95. Ferroni P, Basili S, Falco A, Davì G. Platelet activation in type 2 diabetes mellitus. J Thromb Haemost JTH. 2004 Aug;2(8):1282–91.

96. Patko Z, Császár A, Acsády G, Ory I, Takacs E, Furesz J. Elevation of monocyte-platelet aggregates is an early marker of type 2 diabetes. Interv Med Appl Sci. 2012 Dec 1;4:181–5.

97. del Conde I, Shrimpton CN, Thiagarajan P, López JA. Tissue-factor–bearing microvesicles arise from lipid rafts and fuse with activated platelets to initiate coagulation. Blood. 2005 Sep 1;106(5):1604–11.

98. Yun SH, Sim EH, Goh RY, Park JI, Han JY. Platelet Activation: The Mechanisms and Potential Biomarkers. BioMed Res Int. 2016 Jun 15;2016:e9060143.

99. Harding SA, Sommerfield AJ, Sarma J, Twomey PJ, Newby DE, Frier BM, et al. Increased CD40 ligand and platelet–monocyte aggregates in patients with type 1 diabetes mellitus. Atherosclerosis. 2004 Oct 1;176(2):321–5.

100. Tesch GH. Role of Macrophages in Complications of Type 2 Diabetes. Clin Exp Pharmacol Physiol. 2007;34(10):1016–9.

101. Badlou BA, Wu YP, Smid WM, Akkerman JWN. Platelet binding and phagocytosis by macrophages. Transfusion (Paris). 2006 Aug;46(8):1432–43.

102. Daub K, Langer H, Seizer P, Stellos K, May AE, Goyal P, et al. Platelets induce differentiation of human CD34+ progenitor cells into foam cells and endothelial cells. FASEB J Off Publ Fed Am Soc Exp Biol. 2006 Dec;20(14):2559–61.

103. Tretjakovs P, Kalnins U, Dabina I, Erglis A, Dinne I, Jurka A, et al. Nitric Oxide Production and Arachidonic Acid Metabolism in Platelet Membranes of Coronary Heart Disease Patients with and without Diabetes. Med Princ Pract. 2003 Jan 30;12(1):10–6.

104. Okada AK, Teranishi K, Ambroso MR, Isas JM, Vazquez-Sarandeses E, Lee JY, et al. Lysine acetylation regulates the interaction between proteins and membranes. Nat Commun. 2021 Nov 9;12:6466.

105. Li K, Qiu C, Sun P, Liu D chen, Wu T jun, Wang K, et al. Ets1-Mediated Acetylation of FoxO1 Is Critical for Gluconeogenesis Regulation during Feed-Fast Cycles. Cell Rep. 2019 Mar 12;26(11):2998-3010.e5.

106. Ponugoti B, Kim DH, Xiao Z, Smith Z, Miao J, Zang M, et al. SIRT1 Deacetylates and Inhibits SREBP-1C Activity in Regulation of Hepatic Lipid Metabolism*,. J Biol Chem. 2010 Oct 29;285(44):33959–70.

107. Le-Tian Z, Cheng-Zhang H, Xuan Z, Zhang Q, Zhen-Gui Y, Qing-Qing W, et al. Protein acetylation in mitochondria plays critical functions in the pathogenesis of fatty liver disease. BMC Genomics. 2020 Jun 26;21(1):435.

108. Kim H, Mendez R, Chen X, Fang D, Zhang K. Lysine Acetylation of CREBH Regulates Fasting-Induced Hepatic Lipid Metabolism. Mol Cell Biol. 2015 Dec;35(24):4121–34.

109. Park JM, Jo SH, Kim MY, Kim TH, Ahn YH. Role of transcription factor acetylation in the regulation of metabolic homeostasis. Protein Cell. 2015 Nov;6(11):804–13.

110. Kumar M, Parchani A, Kant R, Das A. Relationship Between Vitamin D Deficiency and Non-alcoholic Fatty Liver Disease: A Cross-Sectional Study From a Tertiary Care Center in Northern India. Cureus. 2023 Feb;15(2):e34921.

111. Coyne D, Acharya M, Qiu P, Abboud H, Batlle D, Rosansky S, et al. Paricalcitol capsule for the treatment of secondary hyperparathyroidism in stages 3 and 4 CKD. Am J Kidney Dis Off J Natl Kidney Found. 2006 Feb;47(2):263–76.

112. Hariri M, Zohdi S. Effect of Vitamin D on Non-Alcoholic Fatty Liver Disease: A Systematic Review of Randomized Controlled Clinical Trials. Int J Prev Med [Internet]. 2019 [cited 2023 Aug 2];10. Available from: https://www.ncbi.nlm.nih.gov/pmc/articles/PMC6360993/

113. Reiter FP, Ye L, Bösch F, Wimmer R, Artmann R, Ziesch A, et al. Antifibrotic effects of hypocalcemic vitamin D analogs in murine and human hepatic stellate cells and in the CCl4 mouse model. Lab Invest. 2019 Dec;99(12):1906–17.

114. Ali TM, El Esawy B, Elaskary A. Effect of paricalcitol on pancreatic oxidative stress, inflammatory markers, and glycemic status in diabetic rats. Ir J Med Sci 1971 -. 2018 Feb 1;187(1):75–84.

115. Wang S, Huang S, Liu X, He Y, Liu Y. Paricalcitol Ameliorates Acute Kidney Injury in Mice by Suppressing Oxidative Stress and Inflammation via Nrf2/HO-1 Signaling. Int J Mol Sci. 2023 Jan 4;24(2):969.

116. Duplancic D, Cesarik M, Poljak NK, Radman M, Kovacic V, Radic J, et al. The influence of selective vitamin D receptor activator paricalcitol on cardiovascular system and cardiorenal protection. Clin Interv Aging. 2013 Feb 15;8:149–56.

117. Sarkar S, Bhattacharya S, Alam MdJ, Yadav R, Banerjee SK. Hypoxia aggravates non-alcoholic fatty liver disease in presence of high fat choline deficient diet: A pilot study. Life Sci. 2020 Nov 1;260:118404.

118. Sanyal D, Mukherjee P, Raychaudhuri M, Ghosh S, Mukherjee S, Chowdhury S. Profile of liver enzymes in non-alcoholic fatty liver disease in patients with impaired glucose tolerance and newly detected untreated type 2 diabetes. Indian J Endocrinol Metab. 2015;19(5):597–601.

119. Lorvand Amiri H, Agah S, Tolouei Azar J, Hosseini S, Shidfar F, Mousavi SN. Effect of daily calcitriol supplementation with and without calcium on disease regression in non-alcoholic fatty liver patients following an energy-restricted diet: Randomized, controlled, double-blind trial. Clin Nutr Edinb Scotl. 2017 Dec;36(6):1490–7.

120. Wei F, Li J, Chen C, Zhang K, Cao L, Wang X, et al. Higher Serum Uric Acid Level Predicts Non-alcoholic Fatty Liver Disease: A 4-Year Prospective Cohort Study. Front Endocrinol [Internet]. 2020 [cited 2023 Aug 9];11. Available from: https://www.frontiersin.org/articles/10.3389/fendo.2020.00179

121. Ahmed OM, Ali TM, Abdel Gaid MA, Elberry AA. Effects of enalapril and paricalcitol treatment on diabetic nephropathy and renal expressions of TNF-α, p53, caspase-3 and Bcl-2 in STZ-induced diabetic rats. Mukhopadhyay P, editor. PLOS ONE. 2019 Sep 17;14(9):e0214349.

122. Marchesini G, Brizi M, Morselli-Labate AM, Bianchi G, Bugianesi E, McCullough AJ, et al. Association of nonalcoholic fatty liver disease with insulin resistance. Am J Med. 1999 Nov;107(5):450–5.

123. Utzschneider KM, Kahn SE. The Role of Insulin Resistance in Nonalcoholic Fatty Liver Disease. J Clin Endocrinol Metab. 2006 Dec 1;91(12):4753–61.

124. Talaei A, Mohamadi M, Adgi Z. The effect of vitamin D on insulin resistance in patients with type 2 diabetes. Diabetol Metab Syndr. 2013 Feb 26;5(1):8.

125. Martin A, Lang S, Goeser T, Demir M, Steffen HM, Kasper P. Management of Dyslipidemia in Patients with Non-Alcoholic Fatty Liver Disease. Curr Atheroscler Rep. 2022 Jul 1;24(7):533–46.

126. Baghel DS, Gaikwad K, Rathore V, Saxena R, Dubey R, Ansari YM. Association of Lipid Profile and Liver Parameters with Different Grades of Non-alcoholic Fatty Liver Disease. Int J Sci Res Dent Med Sci. 2023 Mar 9;5(1):1–6.

127. Kendrick AA, Choudhury M, Rahman SM, McCURDY CE, Friederich M, Van Hove JLK, et al. Fatty liver is associated with reduced SIRT3 activity and mitochondrial protein hyperacetylation. Biochem J. 2011 Feb 1;433(3):505–14.

128. Carnevale I, Pellegrini L, D'Aquila P, Saladini S, Lococo E, Polletta L, et al. SIRT1-SIRT3 Axis Regulates Cellular Response to Oxidative Stress and Etoposide. J Cell Physiol. 2017 Jul;232(7):1835–44.

129. Wu T, Liu Y hua, Fu Y cai, Liu X mu, Zhou X hui. Direct Evidence of Sirtuin Downregulation in the Liver of Non-Alcoholic Fatty Liver Disease Patients. Ann Clin Lab Sci. 2014 Sep 21;44(4):410–8.

130. Li R, Xin T, Li D, Wang C, Zhu H, Zhou H. Therapeutic effect of Sirtuin 3 on ameliorating nonalcoholic fatty liver disease: The role of the ERK-CREB pathway and Bnip3-mediated mitophagy. Redox Biol. 2018 Sep 1;18:229–43.

131. Nogueiras R, Habegger KM, Chaudhary N, Finan B, Banks AS, Dietrich MO, et al. SIRTUIN 1 AND SIRTUIN 3: PHYSIOLOGICAL MODULATORS OF METABOLISM. Physiol Rev. 2012 Jul;92(3):1479–514.

132. Sharma G, Parihar A, Parihar P, Parihar MS. Downregulation of sirtuin 3 by palmitic acid increases the oxidative stress, impairment of mitochondrial function, and apoptosis in liver cells. J Biochem Mol Toxicol [Internet]. 2019 Aug [cited 2023 Aug 4];33(8). Available from: https://onlinelibrary.wiley.com/doi/10.1002/jbt.22337

133. Jiang Y, Chen D, Gong Q, Xu Q, Pan D, Lu F, et al. Elucidation of SIRT-1/PGC-1α-associated mitochondrial dysfunction and autophagy in nonalcoholic fatty liver disease. Lipids Health Dis. 2021 Apr 26;20:40.

134. Nikooyeh B, Hollis BW, Neyestani TR. The effect of daily intake of vitamin D-fortified yogurt drink, with and without added calcium, on serum adiponectin and sirtuins 1 and 6 in adult subjects with type 2 diabetes. Nutr Diabetes. 2021 Jul 30;11(1):1–8.

135. Yang J, Zhang Y, Pan Y, Sun C, Liu Z, Liu N, et al. The Protective Effect of 1,25(OH)2D3 on Myocardial Function is Mediated via Sirtuin 3-Regulated Fatty Acid Metabolism. Front Cell Dev Biol. 2021 Apr 26;9:627135.

136. Feige JN, Auwerx J. Transcriptional targets of sirtuins in the coordination of mammalian physiology. Curr Opin Cell Biol. 2008 Jun;20(3):303–9.

137. Yang H, Zhang W, Pan H, Feldser HG, Lainez E, Miller C, et al. SIRT1 Activators Suppress Inflammatory Responses through Promotion of p65 Deacetylation and Inhibition of NF-κB Activity. PLOS ONE. 2012 Sep 28;7(9):e46364.

138. C B, Km R, T V, Hr O, H R, M F, et al. Functional relevance of novel p300-mediated lysine 314 and 315 acetylation of RelA/p65. Nucleic Acids Res [Internet]. 2008 Mar [cited 2023 Aug 4];36(5). Available from: https://pubmed.ncbi.nlm.nih.gov/18263619/

139. Dong J, Jimi E, Zeiss C, Hayden MS, Ghosh S. Constitutively active NF-κB triggers systemic TNFα-dependent inflammation and localized TNFα-independent inflammatory disease. Genes Dev. 2010 Aug 15;24(16):1709–17.

140. Kalliolias GD, Ivashkiv LB. TNF biology, pathogenic mechanisms and emerging therapeutic strategies. Nat Rev Rheumatol. 2016 Jan;12(1):49–62.

141. Matsuki T, Horai R, Sudo K, Iwakura Y. IL-1 Plays an Important Role in Lipid Metabolism by Regulating Insulin Levels under Physiological Conditions. J Exp Med. 2003 Sep 15;198(6):877–88.

142. Kakino S, Ohki T, Nakayama H, Yuan X, Otabe S, Hashinaga T, et al. Pivotal Role of TNF-α in the Development and Progression of Nonalcoholic Fatty Liver Disease in a Murine Model. Horm Metab Res Horm Stoffwechselforschung Horm Metab. 2018 Jan;50(1):80–7.

143. Kamari Y, Shaish A, Vax E, Shemesh S, Kandel-Kfir M, Arbel Y, et al. Lack of Interleukin-1α or Interleukin-1β Inhibits Transformation of Steatosis to Steatohepatitis and Liver Fibrosis in Hypercholesterolemic Mice. J Hepatol. 2011 Nov;55(5):1086–94.

144. Guo L, Zhang H, Yan X. Protective effect of dihydromyricetin revents fatty liver through nuclear factor-κB/p53/B-cell lymphoma 2-associated X protein signaling pathways in a rat model. Mol Med Rep. 2019 Mar;19(3):1638–44.

145. Kim M, Lee S, Jung N, Lee K, Choi J, Kim SH, et al. The Vitamin D analogue paricalcitol attenuates hepatic ischemia/reperfusion injury through down-regulation of Toll-like receptor 4 signaling in rats. Arch Med Sci. 2016 Jun 1;13.

146. Kang HH, Kim IK, Lee H in, Joo H, Lim JU, Lee J, et al. Chronic intermittent hypoxia induces liver fibrosis in mice with diet-induced obesity via TLR4/MyD88/MAPK/NF-kB signaling pathways. Biochem Biophys Res Commun. 2017 Aug 19;490(2):349–55.

147. Rensen SS, Slaats Y, Nijhuis J, Jans A, Bieghs V, Driessen A, et al. Increased Hepatic Myeloperoxidase Activity in Obese Subjects with Nonalcoholic Steatohepatitis. Am J Pathol. 2009 Oct;175(4):1473–82.

148. Olmos Y, Sánchez-Gómez FJ, Wild B, García-Quintans N, Cabezudo S, Lamas S, et al. SirT1 Regulation of Antioxidant Genes Is Dependent on the Formation of a FoxO3a/PGC-1α Complex. Antioxid Redox Signal. 2013 Nov 1;19(13):1507–21.

149. Rangarajan P, Karthikeyan A, Lu J, Ling EA, Dheen ST. Sirtuin 3 regulates Foxo3a-mediated antioxidant pathway in microglia. Neuroscience. 2015 Dec 17;311:398–414.

150. Tseng AHH, Wu LH, Shieh SS, Wang DL. SIRT3 interactions with FOXO3 acetylation, phosphorylation and ubiquitinylation mediate endothelial cell responses to hypoxia. Biochem J. 2014 Oct 23;464(1):157–68.

151. Wang L, Zhu X, Sun X, Yang X, Chang X, Xia M, et al. FoxO3 regulates hepatic triglyceride metabolism via modulation of the expression of sterol regulatory-element binding protein 1c. Lipids Health Dis. 2019 Nov 15;18(1):197.

152. Boskovic M, Bundalo M, Zivkovic M, Stanisic J, Kostic M, Koricanac G, et al. Estradiol ameliorates antioxidant axis SIRT1-FoxO3a-MnSOD/catalase in the heart of fructose-fed ovariectomized rats. J Funct Foods. 2019 Jan 1;52:690–8.

153. Ighodaro OM, Akinloye OA. First line defence antioxidants-superoxide dismutase (SOD), catalase (CAT) and glutathione peroxidase (GPX): Their fundamental role in the entire antioxidant defence grid. Alex J Med. 2018 Dec 1;54(4):287–93.

154. Delli Bovi AP, Marciano F, Mandato C, Siano MA, Savoia M, Vajro P. Oxidative Stress in Non-alcoholic Fatty Liver Disease. An Updated Mini Review. Front Med. 2021 Feb 26;8:595371.

155. Su LJ, Zhang JH, Gomez H, Murugan R, Hong X, Xu D, et al. Reactive Oxygen Species-Induced Lipid Peroxidation in Apoptosis, Autophagy, and Ferroptosis. Oxid Med Cell Longev. 2019 Oct 13;2019:5080843.

156. Madan K, Bhardwaj P, Thareja S, Gupta SD, Saraya A. Oxidant Stress and Antioxidant Status Among Patients With Nonalcoholic Fatty Liver Disease (NAFLD). J Clin Gastroenterol. 2006 Dec;40(10):930.

157. VanWagner LB, Wilcox JE, Ning H, Lewis CE, Carr JJ, Rinella ME, et al. Longitudinal Association of Non-Alcoholic Fatty Liver Disease With Changes in Myocardial Structure and Function: The CARDIA Study. J Am Heart Assoc. 2020 Feb 18;9(4):e014279.

158. Bornstein AB, Rao SS, Marwaha K. Left Ventricular Hypertrophy. In: StatPearls [Internet]. Treasure Island (FL): StatPearls Publishing; 2023 [cited 2023 Aug 28]. Available from: http://www.ncbi.nlm.nih.gov/books/NBK557534/

159. Lucas E, Vila-Bedmar R, Arcones AC, Cruces-Sande M, Cachofeiro V, Mayor F, et al. Obesity-induced cardiac lipid accumulation in adult mice is modulated by G protein-coupled receptor kinase 2 levels. Cardiovasc Diabetol. 2016 Nov 10;15(1):155.

160. Fudim M, Zhong L, Patel KV, Khera R, Abdelmalek MF, Diehl AM, et al. Nonalcoholic Fatty Liver Disease and Risk of Heart Failure Among Medicare Beneficiaries. J Am Heart Assoc. 2021 Nov 16;10(22):e021654.